MINIREVIEW

Quantifying the overall efficiency of circularly polarized emitters

Lorenzo Arrico,[a] Lorenzo Di Bari[a] and Francesco Zinna*[a]

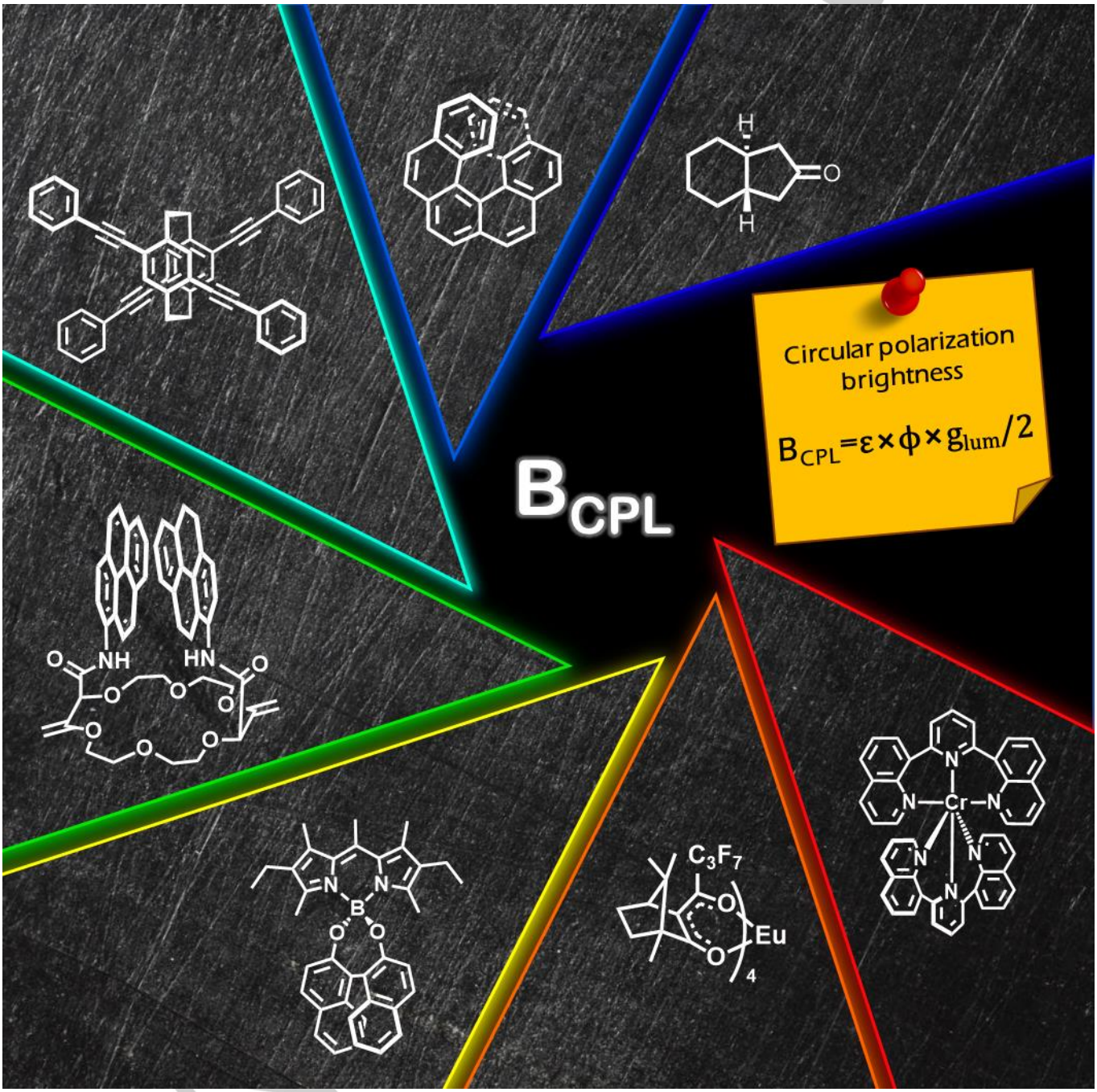

[a] Dr. L. Arrico, Prof. L. Di Bari, Dr. F. Zinna
Dipartimento di Chimica e Chimica Industriale
Università di Pisa
Via Moruzzi 13, 56124,Pisa, Italy
E-mail: francesco.zinna@unipi.it

Abstract: An increasing number of circularly polarized luminescence (CPL) molecular emitters has been developed in the recent years and many of them are intended for applications in which high overall CPL efficiencies are requested. In order to have a complete picture of the efficiency of a CPL emitter, the dissymmetry factor (g_{lum}) is not enough. In the following we propose a new quantity, named CPL brightness (B_{CPL}), which takes into account absorption extinction coefficient and quantum yield along with the g_{lum} factor. We calculated B_{CPL} value for more than 180 compounds reported in the literature and we analyse data distribution for the main classes of CPL molecular emitters. Such tool can be employed to put into context new CPL active compounds and to direct the choice of molecular systems for specific CPL applications.

1. Introduction

Circularly polarized luminescence (CPL), that is the emission of light with a preferential handedness, is a topic gaining more and more interest thanks to the multifarious applications achieved or envisioned.[1] In particular, efficient CPL emitters are needed to obtain circularly polarized (CP) OLEDs (that is electronic devices able to directly emit CP electroluminescence), and some interesting examples are already available in the literature.[2–6] Moreover, CPL emitters are used as probes in (bio)assays, where circular polarization of emitted light adds information which are extremely relevant in inherently chiral environments such as biological media.[7,8] A further development is probably CPL microscopy, where the above-mentioned polarization data can be joined with spatial information.[9] In order to further develop such promising field and its related applications, it is necessary to have a global view of the relative performances of every CPL emitter.

Usually the polarization in emission is quantified by the dissymmetry factor $g_{lum} = 2(I_L-I_R)/(I_L+I_R)$, where I_L and I_R are the left and right CP components of the emission. Usually g_{lum} is calculated on the CPL/emission maximum and, for most organic compounds, it is constant throughout the emission band. For an $i \rightarrow j$ transition, g_{lum} is dependent on the ratio between the transition rotatory strength (R_{ij}) and the transition oscillator strength (D_{ij}):

$$g_{lum} = \frac{4R_{ij}}{|D_{ij}|} = \frac{4|\boldsymbol{\mu_{ij}}| \cdot |\boldsymbol{m_{ji}}| cos\vartheta_{ij}}{|\boldsymbol{\mu_{ij}}|^2 + |\boldsymbol{m_{ji}}|^2}$$

where $\boldsymbol{\mu_{ij}}$ and $\boldsymbol{m_{ji}}$ are the electric and magnetic transition dipole vectors and ϑ_{ij} is the angle between them. In the case of electric dipole-allowed transitions, $|\boldsymbol{\mu_{ij}}| >> |\boldsymbol{m_{ji}}|$, and the previous equation can be approximated as:

$$g_{lum} = \frac{4|\boldsymbol{m_{ji}}| \cos\vartheta_{ij}}{|\boldsymbol{\mu_{ij}}|}$$

With g_{lum} generally << 1.[10–12] Higher g_{lum} factors are achievable with electric dipole forbidden/magnetically allowed transitions, but for the same reasons, only very weak luminescence is observed in these cases, unless other photophysical mechanisms are at play. For most applications, the dissymmetry factor is not sufficient to assess the overall merit of a CPL emitter, as it takes into account only the relative imbalance of CP light in the emission. It is therefore useful to consider also the total photon output over which the polarization is measured.

A widely employed metrics to assess the emission performances and compare different fluorophores is the fluorescence brightness (B),[13] defined as the product of the molar extinction coefficient (ε_λ) measured at the excitation wavelength(λ) and the emission quantum yield (Φ):

$$B = \varepsilon_\lambda \times \phi$$

In analogy with such quantity, we proposed to calculate a brightness for CPL (B_{CPL}) defined as:[14,15]

$$B_{CPL} = \varepsilon_\lambda \times \phi \times \frac{|g_{lum}|}{2} = B \times \frac{|g_{lum}|}{2}$$

This quantity allows one to have an immediate and integrated view of the main photophysical parameters determining the total amount of CP photons emitted by a compound. Moreover, it allows for a direct comparison among molecules and molecular systems belonging to different classes. We note that very recently a similar quantity was proposed by Mori et al. as well.[16,17]

It is worth noting that such definition is only applicable to solution samples. On the other hand, recently Tanner et al.[13] proposed a more general definition of brightness which can be employed even in the case of aggregated, supramolecular and solid-state samples:

$$B' = \xi_{abs} \times \phi$$

where ξ_{abs} is the absorption efficiency, that is the ratio between the number of photons absorbed over the number of incident photons, measurable with an integrating sphere. In this way, CPL brightness for solid-state samples can be calculated analogously to the solution case, as

$$B'_{CPL} = B' \times \frac{|g_{lum}|}{2}$$

In the present review, we shall only consider the simple case of isolated small molecules emitters since a higher number of CPL studies on isolated small molecules have been performed and the parameters to calculate B_{CPL} are easily accessible and therefore available in the literature.

In particular we shall focus on chiral molecules,[18] such as ketones, cyclophanes, BODIPYs, helicenes and helicenoids, pyrene intramolecular excimers, and also on chiral *d*-metal and lanthanide complexes.[10] Within each class of compounds we will discuss what are the major structural characteristics affecting B_{CPL} and what are the parameters which can be controlled (either ε, Φ or g_{lum}) to achieve a bright CPL emitter.

2. CPL emitters

2.1. Ketones

In their seminal work in 1967, Emeis and Oosterhoff[19] described the CPL of the bicyclic ketone **Ket-1**, and later on other examples of CPL from ketones were reported (Scheme 1).[20] In these cases, the CPL is measured for the carbonyl n-π* transition occurring around 400 nm, which draws its rotatory strength from the perturbation induced by the chiral carbon scaffold. Since this transition is magnetically allowed, the g_{lum} factors are relatively high (~10^{-2}) compared to other chiral organic molecules, but in the same time the reported quantum yields and the molar extinction coefficients are very low (10^2 $M^{-1}cm^{-1}$, see Table 1). These values determine in general an extremely low B_{CPL} with a median value of $5.6x10^{-4}$ $M^{-1}cm^{-1}$ (Table 1). As it will be clear later on by the comparison with other CPL active molecules, such values reflect an overall extremely low efficiency of chiral ketones as CPL emitters.

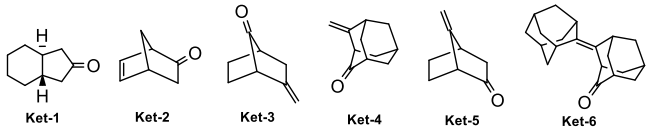

Scheme 1. Structures of CPL-active ketones.

Table 1. Photophysical parameters and B_{CPL} of CPL-active ketones.

Ketones	ε/$M^{-1}cm^{-1}$ (λ_{abs}/nm)	Φx10^3 (λ_{em}/nm)	$\lvert g_{lum}\rvert$ x10^3	B_{CPL} x10^3 /$M^{-1}cm^{-1}$	Ref
Ket-3	140(300)	0.02(400)	3	0.004	20
Ket-2	260(300)	0.05(400)	29.4	0.19	20
Ket-1	30(300)	1(400)	35	0.53	19
Ket-4	110(300)	1.7(400)	6.3	0.59	20
Ket-5	140(300)	0.6(400)	15.7	0.66	20
Ket-6	400(400)	2	12	4.8	20
Average				**1.1**	
Median				**0.56**	

2.2 Cyclophanes

Para-cyclophanes are a versatile scaffold, allowing for various functionalization. In the literature various examples of CPL active cyclophanes are reported (Scheme 2).[21–27] They feature a π-conjugated and rigid structure, which contributes to increase the extinction coefficients and quantum yields allied with the main π-π* transition. In most cases, the surveyed cyclophanes (Scheme 2 and Table 2) display extinction coefficients above 60000 $M^{-1}cm^{-1}$ and quantum yields above 0.5, with their emission maxima falling in the violet-green region (407-517 nm).[21,23–27] The g_{lum} factor is often of the order of 10^{-3}, with a few cases displaying lower (10^{-4}) or higher (10^{-2}) values. These figures result in relatively high B_{CPL} with a median value of 31.9 $M^{-1}cm^{-1}$ and an average of 67.7 $M^{-1}cm^{-1}$.

An interesting trend to observe is that B_{CPL} values significantly increase upon elongation of the core with phenylene ethynylene moieties. This is clearly visible for compounds **Cyp-9**/**Cyp-11**,[17] **Cyp-12**/**Cyp-14**[17] and **Cyp-19**/**Cyp-21**,[26] for which B_{CPL} increases by 5.5, 2.7 and 3.8 times respectively. The increase in B_{CPL} is due to the beneficial effects brought about by conjugation extension on the extinction coefficients and quantum yields, while the g_{lum} factors change only slightly.

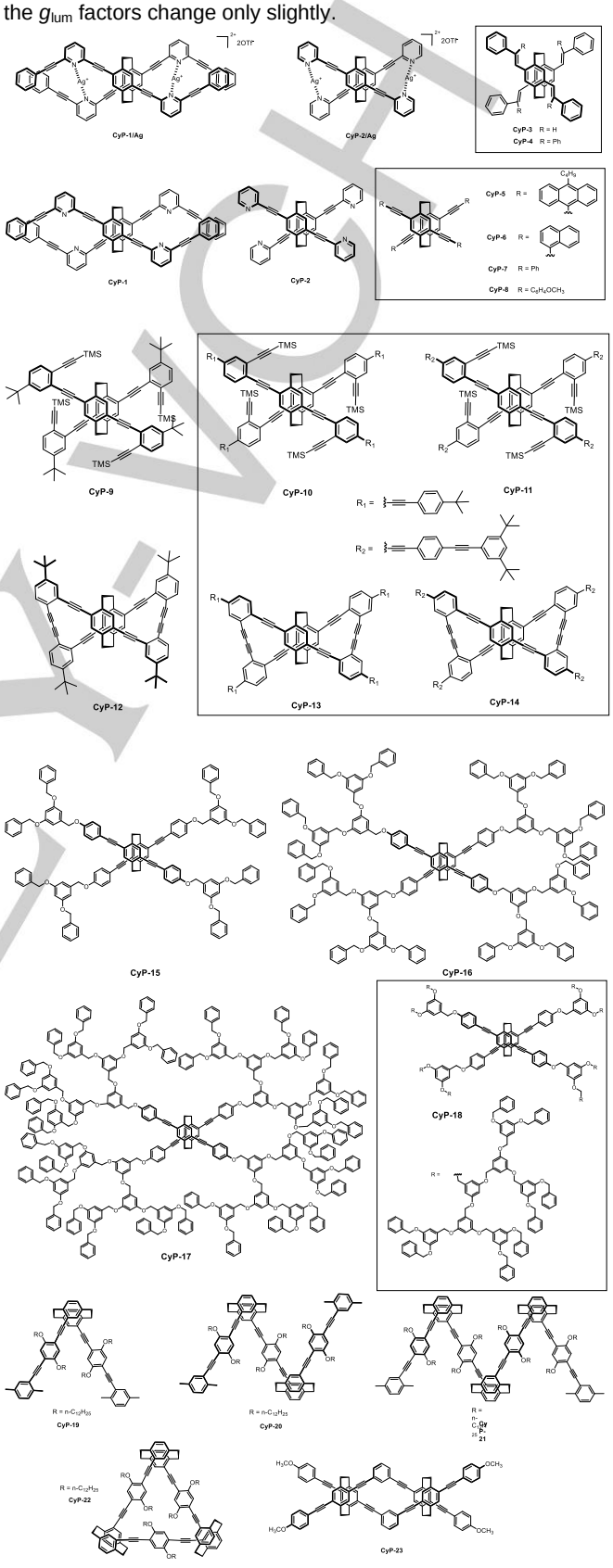

Scheme 2. Structures of CPL-active cyclophanes.

Table 2. Photophysical parameters and B_{CPL} of CPL-active cyclophanes.

Cyclophanes	ε/$M^{-1}cm^{-1}$ (λ_{abs}/nm)	Φ (λ_{em}/nm)	$\lvert g_{lum}\rvert$ x10^3	B_{CPL} /$M^{-1}cm^{-1}$	Ref
Cyp-1/Ag	110000(393)	0.35(421)	0.27	5.2	21
Cyp-4	40000(403)	0.58(494)	0.73	8.5	22
Cyp-5	87000(459)	0.42(503)	0.5	9.1	23
Cyp-9	44000(372)	0.46(418)	1.4	14.2	24
Cyp-7	63000(349)	0.60(412)	1.1	20.8	23
Cyp-2/Ag	70000(378)	0.24(427)	2.5	21.0	21
Cyp-15	67000(363)	0.63(415)	1.4	29.5	25
Cyp-1	90000(356)	0.56(517)	1.2	30.2	21
Cyp-8	68000(361)	0.66(416)	1.4	31.4	25
Cyp-17	68000(365)	0.66(417)	1.4	31,4	25
Cyp-19	70000(374)	0.5(407)	1.8	31,5	26
Cyp-16	69000(364)	0.66(416)	1.4	31.9	25
Cyp-18	68000(363)	0.67(416)	1.4	31.9	25
Cyp-6	79000(380)	0.78(421)	1.6	49.3	23
Cyp-20	100000(375)	0.47(414)	2.1	49,3	26
Cyp-2	60000(342)	0.59(421)	2.8	49,6	21
Cyp-22	80000(364)	0.64(413)	2.2	56.3	26
Cyp-23	140000(379)	0.62(419)	1.5	65.1	27
Cyp-10	141000(398)	0.8(438)	1.2	67.7	24
Cyp-11	179000(403)	0.88(443)	1.0	78.8	24
Cyp-3	60000(395)	0.78(455)	3.7	86.6	22
Cyp-21	160000(376)	0.60(415)	2.5	120.0	26
Cyp-12	46000(391)	0.41(453)	13	122.6	24
Cyp-13	106000(419)	0.6(471)	10	318.0	24
Cyp-14	127000(422)	0.70(474)	7.5	333.4	24
Average				**67.7**	
Median				**31.9**	

2.3 BODIPYs

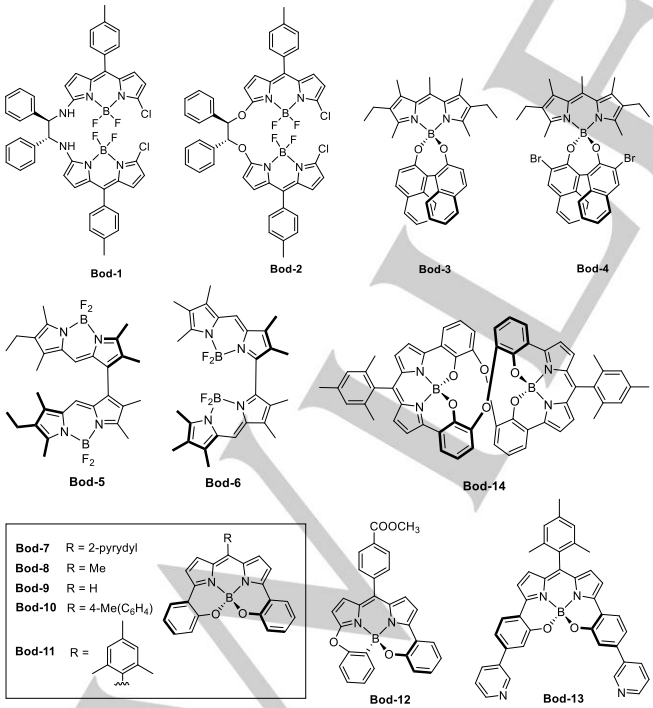

Scheme 3. Structures of CPL-active BODIPYs.

BODIPYs (4-bora-3a,4a-diaza-s-indacene) are a class of compounds showing intense absorption and high quantum yield resulting often in high brightness, moreover their emission wavelengths can be tuned by controlling the core substituents. Such features make them suitable as fluorescent probes for cell imaging.[28] In recent years, various research groups prepared and investigated optically active BODIPYs (Scheme 3).[29–35] A strategy to induce a defined chirality to the BODIPY core is to link 3,5-*ortho*-phenolic substituents to the central boron atom (**Bod-7**/**Bod-11** and **Bod-13**, **Bod-14**),[30,32] or to introduce stereogenic elements as in compounds **Bod-3**/**Bod-4**.[33,35] Moreover, chiral dimeric compounds, such as **Bod-3**/**Bod-6** and **Bod-14**,[29,30,33] are also present in the literature. Overall, chiral BODIPY compounds reported in Scheme 3 and Table 3 show relatively high extinction coefficient and quantum yields (> 0.4 in most cases) with emission maxima in the green-red region (524-678 nm) and g_{lum} factors in the 10^{-3} range. These figures afford B_{CPL} values between 5.8 and 159.2 M^{-1}cm-1, with a median value of 27.2 and an average of 47.0 $M^{-1}cm^{-1}$. Considering **Bod-7**/**Bod-13** series,[30,32] we can notice that the substituents in positions 3,5 and in particular in position 8, affect mainly the quantum yields and, to a lesser extent, extinction coefficients, while they have only a limited impact on the g_{lum} factors. This suggests that B_{CPL} efficiency of chiral BODIPY is largely controlled by their photophysical parameters rather than their chiroptical performances in terms of dissymmetry factor.

Table 3. Photophysical parameters and B_{CPL} of CPL-active BODIPYs.

BODIPYs	ε/$M^{-1}cm^{-1}$ (λ_{abs}/nm)	Φ (λ_{em}/nm)	$\lvert g_{lum}\rvert$ x10^3	B_{CPL} /$M^{-1}cm^{-1}$	Ref
Bod-1	83000(525)	0.14(544)	1	5.8	31
Bod-2	95000(515)	0.16(524)	1	7.6	31
Bod-3	53000(525)	0.44(550)	0.85	9.9	33
Bod-5	78000(552)	0.76(603)	0.4	11.9	29
Bod-7	28190(643)	0.28(675)	4.2	16.6	32
Bod-4	65000(525)	0.69(575)	0.8	17.9	35
Bod-12	30000(593)	0.49(622)	3.7	27.2	34
Bod-10	40000(622)	0.52(637)	4.3	44.7	32
Bod-11	47000(626)	0.72(650)	3	50.8	30
Bod-8	49020(615)	0.73(635)	3.3	59.0	32
Bod-13	67000(643)	0.68(678)	3.3	75.2	30
Bod-9	50760(625)	0.65(632)	4.7	77.5	32
Bod-6	70000(560)	0.71(655)	3.8	94.4	29
Bod-14	61000(631)	0.58(663)	9	159.2	30
Average				**47.0**	
Median				**27.2**	

2.4 Helicenes and helicenoids

Helicenes are polyaromatic molecules presenting *ortho*-fused aromatic units which adopt a helicoidal twist due to steric effects. Helicenes may display an all-carbon skeleton or they may contain some heteroatom in their scaffold (i.e. N, P, S, O, Si and B): hetero[*n*]helicenes (aza[*n*]helicenes, phospha[*n*]helicenes, oxa[*n*]helicenes, and so on). When the π-conjugation is not extended to the entire scaffold, i.e. the helicenic system is not formed only by aromatic units, they are named *helicenoid*s.[36,37]

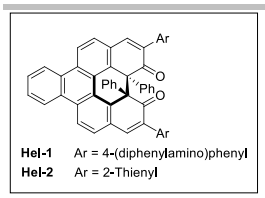


Hel-3

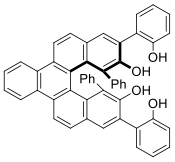
Hel-4

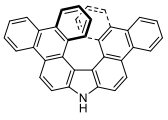
Hel-29


Hel-30

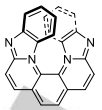
Hel-31

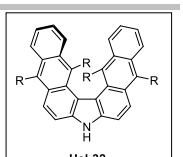
Hel-32 R = Si(*i*-Pr)$_3$

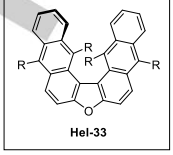
Hel-33

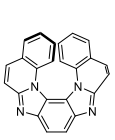
Hel-34

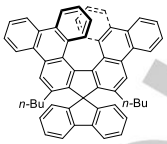
Hel-35

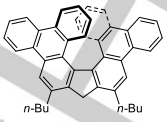
Hel-36

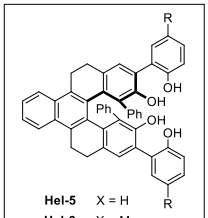
Hel-5 X = H
Hel-6 X = Me
Hel-7 X = F

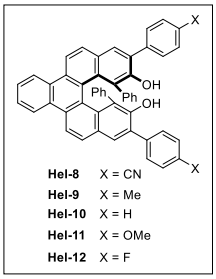
Hel-8 X = CN
Hel-9 X = Me
Hel-10 X = H
Hel-11 X = OMe
Hel-12 X = F

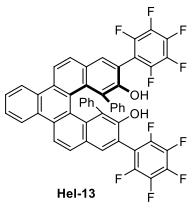
Hel-13

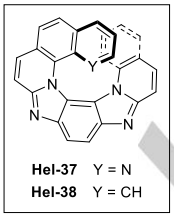
Hel-37 Y = N
Hel-38 Y = CH

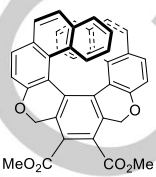
Hel-39

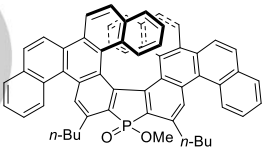
Hel-40

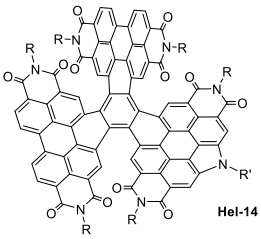
Hel-14

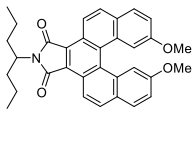
Hel-15

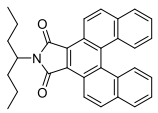
Hel-16

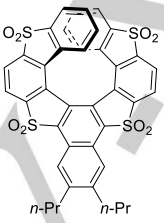
Hel-41

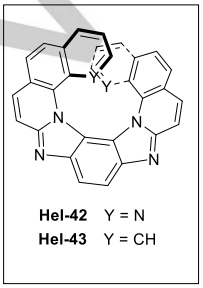
Hel-42 Y = N
Hel-43 Y = CH

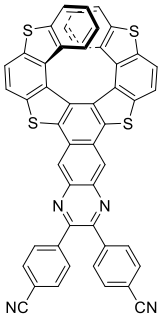
Hel-44

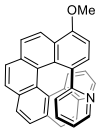
Hel-17

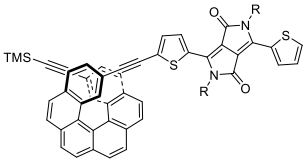
Hel-18

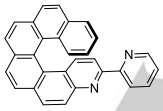
Hel-19

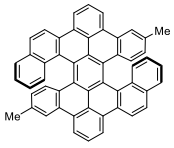
Hel-20

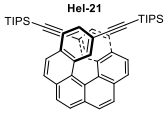
Hel-21

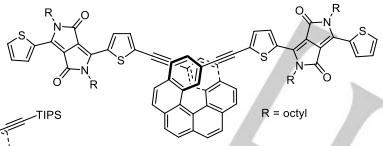
R = octyl
Hel-22

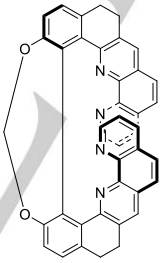
Hel-45

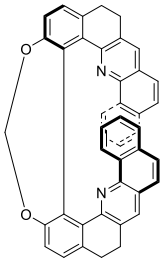
Hel-46

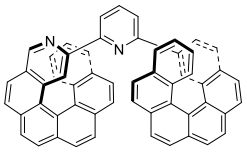
Hel-47

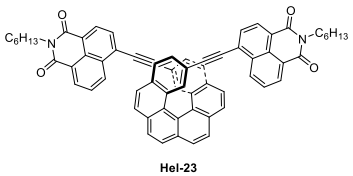
Hel-23

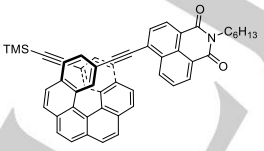
Hel-24

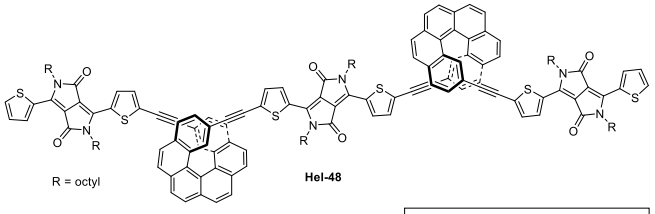
R = octyl
Hel-48

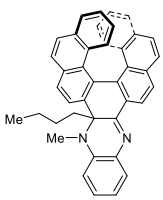
Hel-25

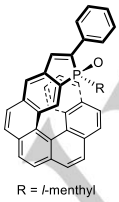
R = *l*-menthyl
Hel-26

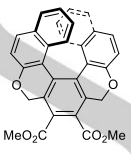
Hel-27


Hel-28

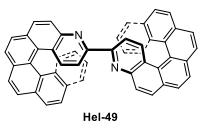
Hel-49

Hel-49

Hel-51 X = N-Ph
Hel-52 X = S

Hel-53 Ar = NMe$_2$
Hel-54 Ar = CN

R = Si(*i*-Pr)$_3$
Hel-55

Hel-56

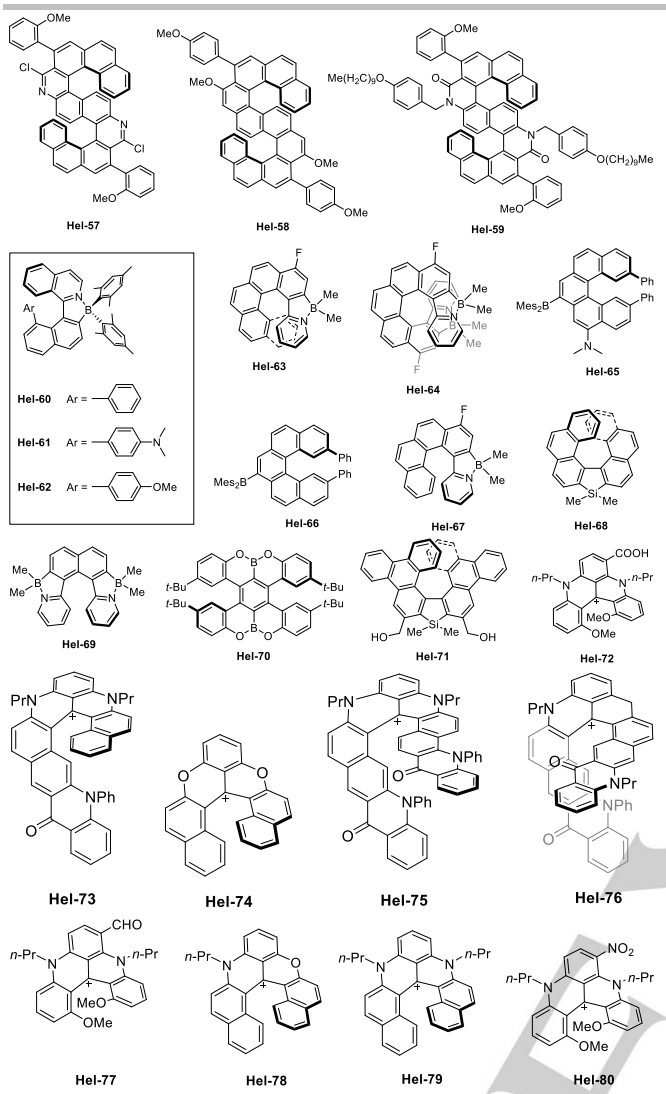

Scheme 4. Structures of CPL-active helicenes and helicenoids.

For simplicity, in the following paragraphs we shall refer to both carbo[*n*]helicenes/helicenoids and hetero[*n*]helicenes/helicenoids with the more general term [*n*]helicene.

Given both the large number of reported CPL-active [*n*]helicenes and also their quite diverse structural motifs (Scheme 4), we shall distinguish and base the discussion of the surveyed compounds on five main classes: 1) purely monomeric organic [*n*]helicenes, (in turn divided into 6 sub-classes according to *n,* with *n* being the number of aromatic units forming the helicene scaffold);[38-65] 2) dimeric systems; [48,50,66–68] 3) S-shaped systems; [69,70] 4) systems with semimetals (B and Si) in the [*n*]helicenes core or directly linked to it; [71–76] and 5) cationic systems[77–80] (Scheme 4 and Table 4).

All the purely monomeric organic systems (**Hel-1** – **Hel-46**) present extinction coefficients in the range 10^4-10^5 M^{-1} cm^{-1} and emission in the violet-green region (maxima between 406-560 nm) in most cases, while more rarely emission maxima fall in the red region (600-610 nm). Concerning [5]helicenes,[38,40–43] the quantum yields are generally between 0.1 and 0.4. The g_{lum} values are in the order of 10^{-4} – 10^{-3}, thus translating into low B_{CPL} values with a median value of 5 M^{-1} cm^{-1} and an average value of 4.9 M^{-1} cm^{-1}. [6]Helicenes[44–50] are a less homogeneous sub-class: compounds with an extended π-conjugation (**Hel-18**, **Hel-20**, **Hel-22**, **Hel-23** and **Hel-24**) present high quantum yields (0.41 – 0.75) [46,47,50], whereas **Hel-17**, **Hel-19** and **Hel-21** have lower quantum yields(< 0.1).[44,45,47–49] In most cases, the g_{lum} factors are similar to those recorded for [5]helicenes, i.e. in the order of 10^{-4} – 10^{-3}, with only **Hel-21**[48,49] being endowed with a higher g_{lum} value ($2.5 \cdot 10^{-2}$). Higher B_{CPL} values were shown by **Hel-23** (45 M^{-1} cm^{-1}) and **Hel-24** (153.9 M^{-1} cm^{-1}),[47] whose high quantum yields (0.7 and 0.45, respectively) are associated to g_{lum} values in the order of 10^{-3}. Comprehensively, the [6]helicenes sub-class presents a median B_{CPL} value of 8.9 M^{-1} cm^{-1} which significantly differs from its average of 29.2 M^{-1} cm^{-1}. Concerning [7]helicenes, the quantum yields are in the range of 0.23 – 0.66,[51,53,55–61] with lower values of 0.1 and 0.06 associated to the phosphahelicene **Hel-26**[52] and to the carbohelicene **Hel-28**,[54] respectively. As for the [5] and [6]helicenes, the g_{lum} factors are in the order of 10^{-4} – 10^{-3}. An exception is observed for triphenylene-based compounds **Hel-35** and **Hel-36** presenting g_{lum} values around $3 \cdot 10^{-2}$.[61] The median B_{CPL} value is 12.9 M^{-1} cm^{-1} and the average 17.4 M^{-1} cm^{-1}. For larger [*n*]helicenes (with *n* = 8, 9 and 11), the quantum yields are generally low (<0.3) and the g_{lum} factors are again in the order of 10^{-4} – 10^{-3}. [53,60,62–65] For *n* = 8 and *n* = 11, the B_{CPL} analysis could be performed only on two cases each, so the median/average values are 4.8 M^{-1} cm^{-1} for [8]helicenes and 1.35 M^{-1} cm^{-1} for [11]helicenes. In the case of [9]helicenes, the median B_{CPL} value is 3 M^{-1} cm^{-1} and the average 14.1 M^{-1} cm^{-1}.

Dimeric systems (**Hel-47** – **Hel-55**) show extinction coefficients in the range 42000-95000 M^{-1} cm^{-1}, with emission maxima falling in the blue-red region (420-650 nm).[48,50,66–68] In most case, the quantum yields are between 0.22 and 0.55. The g_{lum} factors are generally in the range of 10^{-3} – 10^{-2}. Comparing the extinction coefficients of the dimers and the corresponding monomeric units (see **Hel-21** *vs* **Hel-50** – **Hel-54**[48,49]), at least a 3-fold increase is observed. These features translate in quite high B_{CPL} values, e.g. for the compounds **Hel-53** – **Hel-55**, [48,68] which are endowed with B_{CPL} higher than 100 M^{-1} cm^{-1}. Overall, the B_{CPL} median value is 64.8 M^{-1} cm^{-1} and the average is 73.7 M^{-1} cm^{-1}. As a comparison, the B_{CPL} median value for the monomeric [7]helicenes (the highest amongst the purely monomeric organic helicenes, see above) is 5-fold lower than one calculated for the surveyed dimeric systems.

In the case of the S-shaped compounds (**Hel-56 – Hel-59**), the emission is limited to the blue region (454-492 nm).[69,70] Their extinction coefficients are in the range 25000-48000 M^{-1} cm^{-1}. The g_{lum} factors are similar to those of the dimeric systems, i.e. in the order of 10^{-3} – 10^{-2}, but their quantum yields are smaller (<0.2). These features bring to intermediate B_{CPL} values between those of the monomeric [*n*]helicenes and those of the dimeric systems. Indeed, the

median B_{CPL} value is 26 M^{-1} cm^{-1} and the average B_{CPL} value is 30 M^{-1} cm^{-1}.

The compounds with Si and B embedded in the helicene scaffold or directly bound to one of the scaffold aromatic units (**Hel-60** – **Hel-71**) present extinction coefficients in the range of 1000-34000 M^{-1} cm^{-1} and their emission fall in the blue-yellow region (430-586 nm).[71–76] The quantum yields are quite dispersed, going from 0.07 (in the case of **Hel-63** and **Hel-64**[72]) to 0.65 (**Hel-70**[75]), and the g_{lum} factors are generally low (in the order of 10^{-4} – 10^{-3}). However, **Hel-71** presents a higher g_{lum} factor ($1.6 \cdot 10^{-2}$),[76] which in combination with a relatively good quantum yield (0.15) gives rise to the highest B_{CPL} value of this class (40.8 M^{-1} cm^{-1}). Taking into account all the compounds of this sub-class, the median B_{CPL} value is 1.6 M^{-1} cm^{-1} and the average is 6.9 M^{-1} cm^{-1}, which are in line with the values of the purely organic monomeric [*n*]helicenes.

Finally the cationic [*n*]helicenes (**Hel-72** – **Hel-80**) present good extinction coefficients (8000-15500) at longer wavelengths than most of the aforementioned systems.[77–80] This feature goes along with the longest emission wavelengths of all the investigated helicenes (595-663 nm). The quantum yields are in the range 0.12-0.37 and the g_{lum} values are in the range 10^{-3}-10^{-4}, affording a median B_{CPL} value of 1.2 M^{-1} cm^{-1}, similar both to the purely monomeric [*n*]helicenes and to the Si/B helicene compounds.

Overall, monomeric helicenes present generally low values of B_{CPL}, both in the case of purely organic systems (neutral and cationic) and in the case of compounds bearing Si and B. On the contrary, both the fused systems (S-Shaped compounds) and the dimeric systems have higher B_{CPL}, thanks to their generally higher values of g_{lum} factors and extinction coefficients. Globally, helicenes and helicenoids display a median and an average B_{CPL} values of 5.1 and 18.7 $M^{-1}cm^{-1}$ respectively.

Table 4. Photophysical parameters and B_{CPL} of CPL-active helicenes and helicenoids. Median and average BCPL values are calculated for each sub-class and global figures are reported at the end of the table.

Helicenes	ε/$M^{-1}cm^{-1}$ (λ_{abs}/nm)	Φ (λ_{em}/nm)	$\lvert g_{lum} \rvert$ x10^3	B_{CPL} /$M^{-1}cm^{-1}$	Ref
[5]Hel					
Hel-1	8128(436)	0.30(482)	0.2	0.2	38
Hel-2	9332(414)	0.22(518)	0.9	0.9	38
Hel-3	60000(370)	0.018(483)	1.8	1	39
Hel-4	51000(330)	0.19(455)	0.35	1.7	40
Hel-5	55000(305)	0.33(424)	0.29	2.6	40
Hel-8	36000(313)	0.22(416)	0.77	3	41
Hel-6	54000(310)	0.41(425)	0.28	3.1	40
Hel-7	55000(301)	0.39(425)	0.42	4.5	40
Hel-9	37000(305)	0.33(407)	0.9	5.5	41
Hel-13	55000(305)	0.27(408)	0.76	5.6	41
Hel-14	92620(556)	0.11(608)	1.2	6.1	42
Hel-10	59000(304)	0.27(408)	0.89	7.1	41
Hel-11	66000(306)	0.23(409)	1	7.6	41
Hel-15	32000(320)	0.22(500)	2.3	8.1	43
Hel-12	98000(320)	0.35(406)	0.61	10.5	41
Hel-16	28000(330)	0.37(460)	2.4	12.4	43
Average				**4.9**	
Median				**5**	
[6]Hel					
Hel-17	21000(310)	0.03(430)	0.8	0.2	44,45
Hel-18	35000(580)	0.41(610)	0.1	0.7	46
Hel-19	34000(320)	0.08(421)	3.2	4.3	47
Hel-20	30000(350)	0.75(529)	0.75	8.4	47
Hel-21	15000(332)	0.05(437)	25	9.4	48,49
Hel-22	85000(580)	0.41(610)	0.6	10.5	50
Hel-23	41000(420)	0.70(436)	3.2	45.9	47
Hel-24	72000(420)	0.45(436)	9.5	153.9	47
Average				**29.2**	
Median				**8.9**	
[7]Hel					
Hel-25	20000(325)	0.25(560)	0.4	1	51
Hel-26	37200(317)	0.10(449)	0.8	1.2	52
Hel-27	17000(380)	0.23(473)	0.95	1.9	53
Hel-28	65000(345)	0.06(494)	2.2	4.3	54
Hel-29	30000(330)	0.31(428)	1.9	8.8	55
Hel-30	19000(320)	0.39(417)	3	11.1	56
Hel-31	8400(416)	0.39(473)	9	14.7	57
Hel-32	28000(500)	0.36(560)	3	15.1	58
Hel-33	45000(500)	0.66(550)	1.2	17.8	59
Hel-34	17000(337)	0.58(456)	7.6	37.6	60
Hel-35	9800(273)	0.30(449)	32	47	61
Hel-36	10000(364)	0.32(428)	30	48	61
Average				**17.4**	
Median				**12.9**	
[8]Hel					
Hel-37	2400(381)	0.15(494)	8	2	60
Hel-38	10000(365)	0.19(488)	8	7.6	60
Average				**4.8**	
Median				**4.8**	
[9]Hel					
Hel-39	7000(388)	0.18(547)	1.1	0.7	53
Hel-40	60000(315)	0.085(501)	0.48	1.2	62
Hel-41	11000(355)	0.27(430)	0.87	1.3	63
Hel-42	5800(342)	0.06(546)	27	4.7	60
Hel-43	21000(335)	0.16(492)	20	33.6	60
Hel-44	110000(400)	0.26(600)	3	42.9	64
Average				**14.1**	
Median				**3**	
[11]Hel					
Hel-45	60000(290)	0.002(437)	8	0.5	65
Hel-46	40000(290)	0.014(420)	8	2.2	65
Average				**1.35**	
Median				**1.35**	
Dimers					
Hel-47	60000(322)	0.08(421)	8.5	20.4	66
Hel-48	95000(580)	0.35(650)	0.9	15	50
Hel-49	42000(330)	0.22(420)	4.8	22.2	67
Hel-50	50000(340)	0.11(424)	20	55	48
Hel-51	60000(323)	0.27(507)	8	64.8	48
Hel-52	58000(318)	0.25(454)	12	87	48
Hel-53	71000(318)	0.28(455)	12	119.3	48
Hel-54	91000(310)	0.28(456)	10	127.4	48

Hel-55	65000(536)	0.55(588)	8.5	151.9	68
Average				**73.7**	
Median				**64.8**	
S-shaped					
Hel-56	27000(358)	0.076(466)	1.5	1.5	69
Hel-57	48000(329)	0.09(454)	11	23.8	70
Hel-58	190000(358)	0.11(464)	2.7	28.2	69
Hel-59	25000(448)	0.19(492)	28	66.6	70
Average				**30**	
Median				**26**	
Si/B					
Hel-60	8200(414)	0.29(495)	0.25	0.3	71
Hel-63	25500(324)	0.07(442)	0.7	0.6	72
Hel-61	4000(433)	0.13(586)	3.5	0.9	71
Hel-62	7400(420)	0.30(502)	0.95	1.1	71
Hel-64	31200(337)	0.07(473)	1	1.1	72
Hel-65	2500(444)	0.19(558)	6.5	1.5	73
Hel-66	1100(422)	0.51(445)	6.3	1.8	73
Hel-67	30400(307)	0.21(430)	0.9	2.9	72
Hel-68	20000(300)	0.23(450)	3.5	8	74
Hel-69	18100(342)	0.49(430)	2.3	10.2	72
Hel-70	25000(411)	0.65(436)	1.7	13.8	75
Hel-71	34000(300)	0.15(482)	16	40.8	76
Average				**6.9**	
Median				**1.6**	
Cationic					
Hel-72	11300(590)	0.29(654)	0.5	0.8	77
Hel-73	12500(615)	0.29(653)	0.1	0.2	78
Hel-74	15500(562)	0.12(595)	0.37	0.3	79
Hel-75	9000(625)	0.25(663)	0.6	0.7	78
Hel-76	8000(615)	0.21(656)	1.4	1.2	78
Hel-77	10750(583)	0.37(640)	0.9	1.8	80
Hel-78	10700(562)	0.22(614)	2.1	2.5	79
Hel-79	14700(614)	0.31(658)	1.1	2.5	79
Hel-80	12000(575)	0.35(624)	1.7	3.6	80
Average				**1.5**	
Median				**1.2**	
Global average				**18.7**	
Global median				**5.1**	

2.5 Pyrene excimers

Excimer emission stems from an excited state dimer formed between monomers which are non-bonding in the ground state. This peculiar emission mechanism has the effect that the emitting state geometry can be significantly different from the ground state one. In chiral molecules, this means that, in contrast to most cases treated so far,[81] excimer-related g_{lum} is not related to absorption dissymmetry factor (g_{abs}). Indeed, a recent literature survey showed that in most cases excimer-related g_{lum} is one or two orders of magnitude higher than the g_{abs} associated with most red-shifted Cotton effect.[82] In particular, pyrene can give rise to efficient excimer generation usually well-separated from monomer localized emission.[83] In this section, we shall take into account compounds consisting of a chiral scaffold mounting pyrene moieties and displaying intramolecular excimer CPL (Scheme 5 and Table 5). Typically, pyrene excimer emission can be obtained by exciting the S_0-S_2 transition around 345-365 nm, such transition has an extinction coefficient in order of 10^4 $M^{-1}cm^{-1}$ per pyrene unit, allowing for an efficient excitation. In most cases, a quantum yield above 0.2 with an allied g_{lum} of 10^{-3}-10^{-2} is obtained.[84–89] In this way, pyrene excimer emission in chiral compounds display a median B_{CPL} values of 43.2 $M^{-1}cm^{-1}$, the highest among organic compounds. A closer look to analogous series, e.g. **Exc-5**/**Exc-7** where pyrene moieties are linked to binaphthyl scaffolds through flexible chains,[84] reveals that the increase in B_{CPL} (from 8.4 to 16.7 $M^{-1}cm^{-1}$) is mostly due to the increase in g_{lum} factor, while the variations in extinction coefficients and quantum yields are minor, suggesting that g_{lum} factors, and therefore B_{CPL} values, are mainly affected by the molecular geometry. On the other hand, It is interesting to consider **Exc-13**/**Exc-15** series,[89] where the pyrene units are linked directly to the binaphthyl/tetranaphtyl scaffold via an ester bond, thus providing a rigid geometry. B_{CPL} value increases more than proportionally with respect to the number of pyrene units moving from **Exc-13** to **Exc-14**, thanks to an allied increase of both extinction coefficient and g_{lum} factor, and it increases only proportionally from **Exc-14** to **Exc-15**, as the extinction coefficient continues to increase whereas g_{lum} factor is only slightly affected. Overall, **Exc-13**/**Exc-15** display the highest B_{CPL} values in the pyrene excimers class (171.6, 577.2, 722.5 $M^{-1}cm^{-1}$ respectively). The beneficial effect of suitable rigid scaffolds on B_{CPL} values is also shown by compounds **Exc-9**/**Exc-11**,[87] where pyrene moieties are linked to different macrocyclic rings via amide bonds. Notably, **Exc-9** was the first organic compound able to emit circularly polarized electrochemiluminescence.[90]

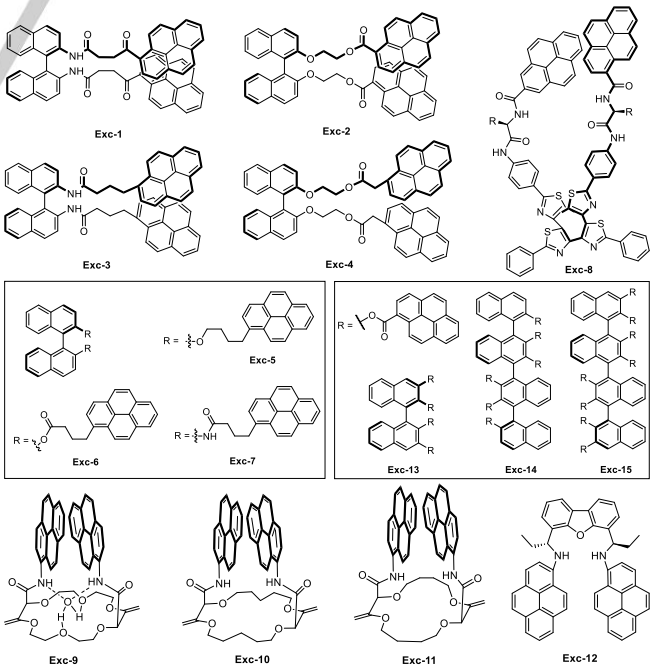

Scheme 5. Structures of compounds displaying pyrene excimer CPL.

Table 5. Photophysical parameters and B_{CPL} of compounds displaying pyrene excimer CPL.

Excimers	ε/M^{-1}cm^{-1} (λ_{abs}/nm)	Φ (λ_{em}/nm)	$\lvert g_{lum}\rvert$ x10^3	B_{CPL} /M^{-1}cm^{-1}	Ref
Exc-1	12000(355)	0.06(513)	6.8	2.4	85
Exc-5	70000(345)	0.20(470)	1.2	8.4	84
Exc-6	70000(345)	0.22(470)	1.5	11.6	84
Exc-8	70000(365)	0.4(500)	10	14	86
Exc-7	70000(345)	0.17(470)	2.8	16.7	84
Exc-2	23000(355)	0.27(513)	6.0	18.6	85
Exc-3	55000(345)	0.25(470)	4.5	30.9	85
Exc-9	40000(345)	0.24(495)	9	43.2	87
Exc-12	40000(410)	0.60(500)	3.9	46.8	88
Exc-4	55000(345)	0.25(470)	6.9	47.4	85
Exc-10	30000(345)	0.46(495)	10	69.0	87
Exc-11	45000(345)	0.32(495)	17	122.4	87
Exc-13	110000(360)	0.24(540)	13	171.6	89
Exc-14	130000(360)	0.24(540)	37	577.2	89
Exc-15	170000(360)	0.25(540)	34	722.5	89
Average				**126.9**	
Median				**43.2**	

2.6 d-metal based compounds

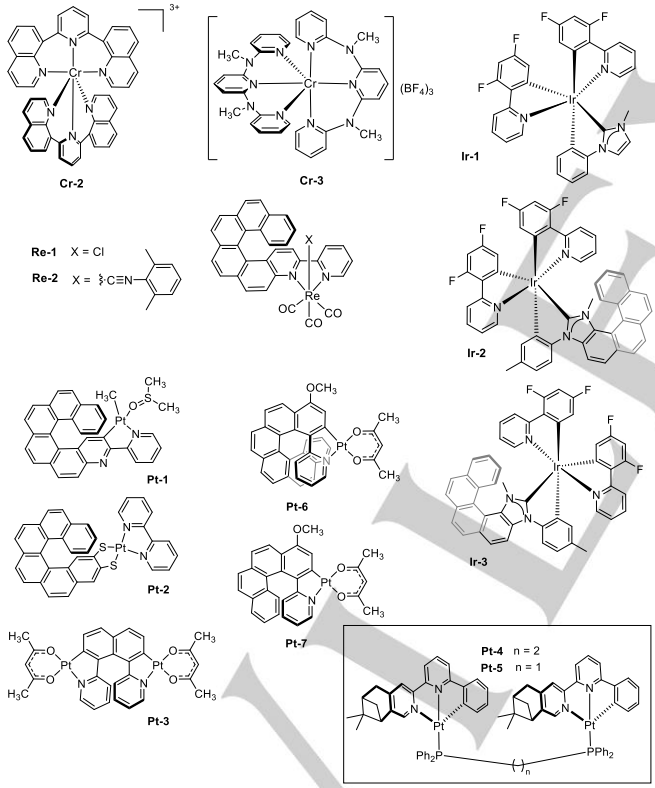

Scheme 6. Structures of CPL-active d-metal compounds.

Table 6. Photophysical parameters and B_{CPL} of CPL-active d-metal compounds. Median and average B_{CPL} values are calculated for each sub-class corresponding to different metals and global figures are reported at the end of the table.

d-metal compounds	ε/M^{-1}cm^{-1} (λ_{abs}/nm)	Φ (λ_{em}/nm)	$\lvert g_{lum}\rvert$ x10^3	B_{CPL} /M^{-1}cm^{-1}	Ref
Cr					
Cr-1	75(458)	6x10^{-5}(672)	28	6.3x10^{-5}	19,91
Cr-2	20000(385)	0.052(750)	200	104	92
Cr-3	30000(300)	0.3(775)	93	418.5	93
Average				**174.2**	
Median				**104**	
Ru					
Ru-1	14000(450)	0.063(625)	0.7	0.31	94,95
Ru-2	18000(444)	0.058(604)	0.7	0.37	96,97
Average				**0.34**	
Median				**0.34**	
Re					
Re-1	10000(440)	0.002(673)	3	0.03	44
Re-2	6000(440)	0.06(598)	1.4	0.25	44
Average				**0.14**	
Median				**0.14**	
Ir					
Ir-1	4810(390)	0.29(498)	0.9	0.63	98
Ir-2	6670(403)	0.13(526)	1.5	0.65	98
Ir-3	6560(402)	0.09(525)	3.7	1.1	98
Average				**0.79**	
Median				**0.65**	
Pt					
Pt-1	5800(429)	0.004(547)	1.1	0.01	45
Pt-2	3640(562)	0.15(715)	0.3	0.08	99
Pt-3	6640(471)	0.13(633)	0.5	0.22	46
Pt-4	1800(420)	0.15(563)	4	0.54	100
Pt-6	5320(467)	0.06(648)	4.5	0.72	46
Pt-5	3300(423)	0.11(638)	4	0.73	100
Pt-7	7800(452)	0.19(644)	12	4.7	46
Average				**1.0**	
Median				**0.54**	
Global average				**29.7**	
Global median				**2.6**	

Chiral coordination compounds containing d-metals able to emit light following metal/ligand charge transfer processes have been investigated as well as CPL emitters. The most commonly reported compounds employ Cr(III),[19,92,93] Ru(II),[94,96] Re(I),[44] Ir(III)[98] and Pt(II) (Scheme 6 and Table 6).[45,46,99,100] The first example was $[Cr(en)_3]^{3+}$ (**Cr-1**, en = ethylenediamine), reported by Emeis and Oosterhoff in 1967.[19] Such compound displayed a relatively high g_{lum} (0.028) but low extinction coefficient and quantum yields. More recently, two more Cr-compounds based on chelating ligands forming bis-tridentate Cr(III) helices were reported.[92,93] This molecular design affords higher extinction coefficients and quantum yields and g_{lum} factors in the order of 10^{-1}, which results in exceptionally high B_{CPL} (104 and 418.5 M^{-1}cm^{-1} for **Cr-2** and **Cr-3** respectively), with emission in the near infrared region. Other renown examples of d-metal CPL emitters are provided by Ru(II) complexes. In particular, $Ru(bipy)_3^{2+}$ (**Ru-1**, bipy = bipyridyl) and $Ru(phen)_3^{2+}$ (**Ru-2**, phen = 1,10-phenanthroline) displays a B_{CPL} around 0.3 M^{-1}cm^{-1}, as a result of rather low quantum yields and g_{lum} factors. It is worth noting that Ru(II) compounds were also proposed as circularly polarized electrochemiluminescent emitters.[94,101] Some examples of

Re(I), Pt(II) and Ir(III) CPL active compounds are reported, with many of them employing helicene-like scaffolds as the ligands. Most of them display B_{CPL} below 1 $M^{-1}cm^{-1}$, but despite this, both Pt and Ir compounds were successfully employed as emitters in CP-OLEDs.[6]

2.7 Lanthanide complexes

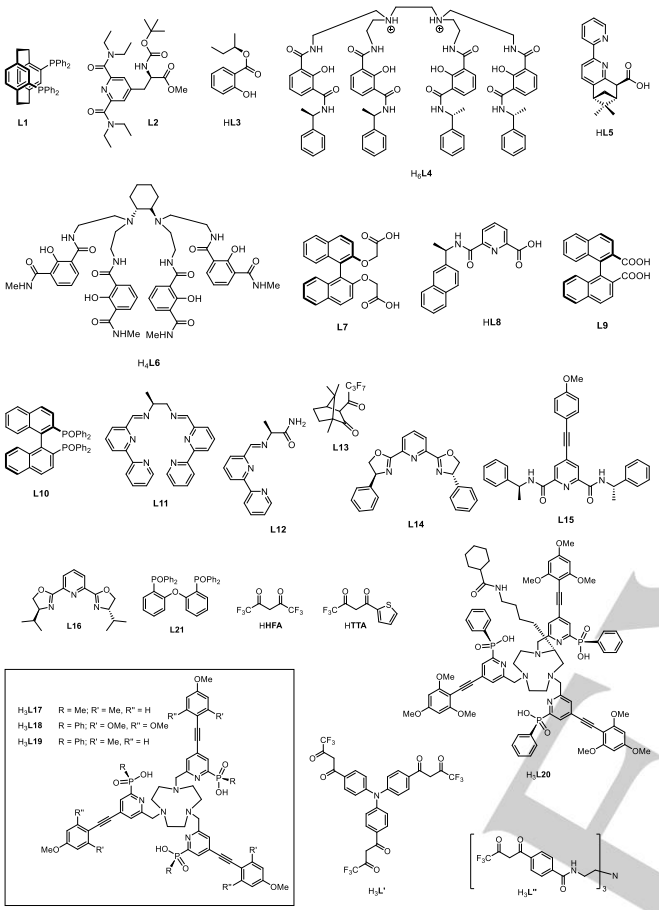

Scheme 7. Structures of ligands employed in CPL-active lanthanides.

The circularly polarized luminescence of trivalent lanthanide ions (Ln^{3+}) in chiral complexes is allied to the *f-f* transitions of the specific Ln^{3+}, and it is therefore a lanthanide-centred property. Generally, thanks to the peculiar features of the 4*f* orbitals, the emission spectra of lanthanide complexes consist of narrow optical bands whose energies are not largely affected by the coordination environment. As a consequence, each lanthanide ion is characterized by specific emission bands. However, since the extinction coefficients of *f-f* transitions are extremely weak (< 10 M^{-1} cm^{-1}) due to Laporte rule, usually the Ln^{3+} emission is promoted *via* an indirect mechanism (the so-called *antenna effect*): upon light absorption by the ligands, usually through an allowed π-π^* transition, the energy is transferred to a Ln^{3+}-centred emissive state.[102] If the ligand is suitably chosen, such process can be extremely efficient, resulting in high complex quantum yield, and therefore high brightness. Given the mechanism, absorption and electronic circular dichroism spectra of chiral lanthanide complexes are dominated by the ligands transition, while emission and CPL spectra are dominated by Ln^{3+} transitions. For this reason, there is no direct relationship between the ligand-centred absorption dissymmetry factors and the g_{lum} values. In comparison to most organic or d-metal compounds, thanks to the magnetically allowed character of most transitions, lanthanide complexes present a very high degree of circular polarization of the emitted light,[10] often reaching values in the order of 10^{-2} - 10^{-1} (with the exceptional value of 1.38 recorded for CsEu(**L13**)$_4$,[103,104] Scheme 7 and Table 7-9).

The energy levels of the lanthanide ions are denoted by the term symbols $^{2S+1}L_J$, where S represents the total electron spin angular momentum, L the total orbital angular momentum and J the total angular momentum. The states with J > 0 present additional sub-levels (the so-called *Stark levels*), so that each state may be composed of a manifold with up to 2J + 1 sub-levels (for integer values of J) or J + ½ sub-levels (for half-integer J values).

For these reasons, in order to perform the B_{CPL} analysis, one must take into account that the emission spectra of lanthanide complexes present several sharp bands, in contrast to what generally observed for other molecules. Usually the quantum yield of a complex is measured by integrating on the whole transitions, thus, when calculating the B_{CPL} for a particular transition, one needs to take into account also the so-called *branching ratio* (β, 0 ≤ β ≤ 1). In this way, only the photons emitted by that specific transition are considered:

$$\beta_i = \frac{I_i}{\sum_j I_j}$$

Where I_i is the integrated intensity of the considered transition and $\sum_j I_j$ is the summation of the integrated intensities over all the transitions. β_i depends on the symmetry and nature of the complex. With this parameter, B_{CPL} calculated for a selected lanthanide transition has to be corrected as follows:

$$B_{CPL} = \beta_i \times \varepsilon_\lambda \times \phi \times \frac{|g_{lum}|}{2} = \beta_i \times B \times \frac{|g_{lum}|}{2}$$

In this case, g_{lum} is the dissymmetry factor associated to the considered transition.

In the case of Tb^{3+} complexes, the emission spectra show bands associated to the transition from the $^5D_4$ emissive state to the ^7F_J ground state levels (J = 0 – 6). Generally, high g_{lum} values are obtained for the $^5D_4 \rightarrow {}^7F_5$ transition centred at ~540 nm. For this reason, in Table 7 only the g_{lum} values of this transition are listed. The surveyed Tb^{3+} complexes[105–109] present extinction coefficients in the range of 23000-75000 M^{-1} cm^{-1} and in most cases the g_{lum} values are in the order of 10^{-2}. $^5D_4 \rightarrow {}^7F_5$ transition is usually the most intense one, giving rise to the typical green emission of Tb. This is reflected by the associated branching ratios, falling in the range between 0.46 and 0.67. With the exception of Tb**L1**(HFA)$_3$ (hexafluoroacetylacetonate) and [Tb**L2**]$^{3+}$,[105] which present low quantum yields and low g_{lum} values, in all the other cases the B_{CPL} values are quite high (94.1 – 306.8 $M^{-1}cm^{-1}$). Comprehensively for Tb compounds, the median B_{CPL} value is 144.4 $M^{-1}cm^{-1}$ and the average 146.4 M^{-1} cm^{-1}.

Luminescent Eu^{3+} complexes generally present several emission bands associated to the transitions from the $^5D_0$ excited state to the ^7F_J ground state levels, with J = 0 – 6, falling in the orange-red region. Thanks to the high quantum yield that can be achieved with suitable antenna ligands and the high g_{lum} achievable for certain transitions when proper chiral ligands are employed, Eu^{3+} compounds are the most commonly investigated in the field of lanthanide-based CPL emitters. Indeed, Eu^{3+} $^5D_0 \rightarrow {}^7F_1$ transition (~590 nm) is endowed with peculiar electronic and magnetic characteristics, generally leading to very high g_{lum} factors.[110] Another important transition, which is generally the most intense one in term of total emission (high β) is the $^5D_0 \rightarrow {}^7F_2$ centred at ~615 nm. In this contribution, whenever possible, both the transitions were examined and the corresponding values reported in Table 8. The complexes present extinction coefficients in the range 11000-80000 M^{-1} cm^{-1},[103,104,116–118,107–109,111–115] except for Eu_4(**L21**)$_4$(**L'**)$_4$ and Eu_4(**L10**)$_4$(**L'**)$_4$, which show extinction coefficients of 600000 M^{-1} cm^{-1} and 800000 M^{-1} cm^{-1}, respectively.[119] In combination with their high quantum yields (0.68 for Eu_4(**L21**)$_4$(**L'**)$_4$ and 0.81 for Eu_4(**L10**)$_4$(**L'**)$_4$), they are endowed with outstanding B_{CPL} values (1122 M^{-1} cm^{-1} and 3240 $M^{-1}cm^{-1}$ respectively) for the $^5D_0 \rightarrow {}^7F_1$ transition. As for the rest, the quantum yields are in the range of 0.1 – 0.55 with few compounds with lower quantum yields. Higher g_{lum} values are almost always observed for the $^5D_0 \rightarrow {}^7F_1$ transition as opposed to the $^5D_0 \rightarrow {}^7F_2$ one (10^{-1} *vs* 10^{-3} – 10^{-2}). On the other hand, the branching ratios follow the opposite trend, with values around 0.1 for the $^5D_0 \rightarrow {}^7F_1$ transition and around 0.6 for the $^5D_0 \rightarrow {}^7F_2$ one (which gives the typical red colour to the Eu^{3+} emission). These features bring to only a slightly higher median B_{CPL} value of the $^5D_0 \rightarrow {}^7F_1$ (86.6 M^{-1} cm^{-1}) with respect to one of the $^5D_0 \rightarrow {}^7F_2$ transition (54.5 M^{-1} cm^{-1}). It should be noted that the majority of the surveyed complexes presents at least one enantiopure ligand. This is not true for Eu**L17**, Eu**L18**, Eu**L19** and Eu(**L21**)$_4$(**L'**)$_4$. For the first three complexes, being the phosphorus chirality labile, both enantiomers are formed upon complexation to Eu^{3+}, namely *R,R,R-Λ-δ,δ,δ,* and *S,S,S-Δ-λ,λ,λ*, where *R* (*S*) is the P chirality, *Λ* (*Δ*) is the chirality of the helical axis and *δ (λ)* is the chirality of the three ring NCCN chelates. Therefore, the enantiopure forms were obtained upon chiral HPLC resolution. In the case of Eu(**L21**)$_4$(**L'**)$_4$, the complex was obtained by substituting the chiral ligand **L10** with the achiral **L21**: the prevalence of one enantiomer over the other was achieved thanks to a chiral memory effect.

Yb^{3+} emission entirely falls in the near-infrared (NIR) region (~980 nm) presenting only the $^2F_{5/2} \rightarrow {}^2F_{7/2}$ transition. So far, very few examples of Yb^{3+}-centred CPL activity have been reported,[120–122] therefore the B_{CPL} analysis could be performed only on two complexes bearing β-diketonates (TTA, thenoyltrifluoroacetonate) as sensitizing ligands (Table 9).[121] Given their low quantum yields (<0.01) the B_{CPL} values are accordingly moderate (2.5 M^{-1} cm^{-1} for Yb**L14**(TTA)$_3$ and 5.2 M^{-1} cm^{-1} for Yb**L16**(TTA)$_3$), even if their g_{lum} values are in line with the g_{lum} values recorded for Tb^{3+} and for the $^5D_0 \rightarrow {}^7F_2$ Eu^{3+} transition, i.e. in the order of 10^{-2}. Anyway, it is worth noting that to date examples of NIR CPL emitters are extremely rare.

Table 8. Photophysical parameters and B_{CPL} of CPL-active Tb-based compounds.

Tb	ε/$M^{-1}cm^{-1}$ (λ_{abs}/nm)	Φ	$\lvert g_{lum}\rvert$ (λ/nm)	β	B_{CPL} /$M^{-1}cm^{-1}$	Ref
Tb**L1**(HFA)$_3$	29000 (300)	0.02	0.008 (544)	0.67	1.5	105
[Tb(**L2**)$_3$]$^{3+}$	75000 (210)	0.012	0.02 (~540)	0.48	4.3	105
[Tb$_9$(**L3**)$_{16}$(μ-OH)$_{10}$]$^+$	60000 (340)	0.14	0.04 (~540)	0.56	94.1	106
[Tb(H$_2$**L4**)]$^+$	23000 (350)	0.63	0.048 (543)	0.56	194.7	107
[Tb$_3$(**L5**)$_6$]$^{2+}$	80000 (310)	0.15	0.081 (~540)	0.57	277	108
Tb(H**L6**)	28200 (303)	0.57	0.083 (543)	0.46	306.8	109
Average					**146.4**	
Median					**144.4**	

Table 8. Photophysical parameters and B_{CPL} of CPL-active Eu-based compounds

Eu	ε/$M^{-1}cm^{-1}$ (λ_{abs}/nm)	Φ	^7F_J	$\lvert g_{lum}\rvert$ (λ/nm)	β	B_{CPL} /$M^{-1}cm^{-1}$	Ref
Eu**L7**(HFA)$_3$	25000 (300)	0.06	J=1	0.013 (594)	0.07	0.7	111
			J=2	0.0015 (613)	0.86	1	
Eu(**L8**)$_3$	11000 (270)	0.006	J=1	0.16 (589)	0.25	1.3	112
			J=2	0.09 (614)	0.58	1.7	
Eu**L9**(HFA)$_3$	25000 (300)	0.13	J=1	0.013 (592)	0.08	3.4	111
			J=2	0.0012 (614)	0.88	1.7	
Eu(H**L6**)(H$_2$O)	19000 (341)	0.07	J=1	0.12 (594)	0.11	9.7	109
			J=2	-	-	-	
Eu**L10**(**L''**)	30000 (335)	0.33	J=1	0.072 (~585)	0.04	14.3	118
			J=2	-	-	-	
[Eu**L11**]$^{3+}$	20000 (310)	0.19	J=1	0.12 (595)	0.13	29.6	113
			J=2	0.04 (~615)	0.61	46.4	
[Eu**L12**]$^{3+}$	12000 (310)	0.45	J=1	0.13 (592)	0.1	35.1	113
			J=2	0.025 (~615)	0.74	50	
[Eu(H$_2$**L4**)]$^+$	23000 (350)	0.11	J=1	0.3 (596)	0.12	45.5	107
			J=2	-	-	-	
CsEu(**L13**)$_4$	35000 (310)	0.03	J=1	1.38 (595)	0.07	50.7	103,104
			J=2	0.25 (614)	0.45	59.1	
Eu**L14**(TTA)$_3$	35000 (345)	0.5	J=1	0.11 (595)	0.09	86.6	114
			J=2	0.01 (614)	0.74	64.7	

$[Eu_3(\mathbf{L5})_6]^{2+}$	80000 (303)	0.13	J=1	0.088 (~590)	0.22	100.7	108
			J=2	0.058 (~615)	0.57	171.9	
$[Eu(\mathbf{L15})_3]^{3+}$	55000 (365)	0.11	J=1	0.26 (595)	0.13	102	115
			J=2	0.11 (616)	0.64	213	
Eu**L16**$(TTA)_3$	27000 (345)	0.4	J=1	0.24 (595)	0.08	103.7	114
			J=2	0.02 (614)	0.78	84.2	
Eu**L17**	65000 (342)	0.54	J=1	0.11 (599)	0.06	116	116
			J=2	-	-	-	
Eu**L18**	65000 (356)	0.5	J=1	0.12 (599)	0.06	117	116
			J=2	-	-	-	
Eu**L20**	55000 (360)	0.55	J=1	0.11 (598)	0.08	133.1	117
			J=2	-	-	-	
Eu**L19**	65000 (343)	0.46	J=1	0.15 (599)	0.06	134.5	116
			J=2	-	-	-	
$Eu_4(\mathbf{L21})_4(\mathbf{L'})_4$	600000 (380)	0.68	J=1	0.11 (592)	0.05	1122	119
			J=2	-	-	-	
$Eu_4(\mathbf{L10})_4(\mathbf{L'})_4$	800000 (380)	0.81	J=1	0.2 (592)	0.05	3240	119
			J=2	-	-	-	
Average			J=1			**286.6**	
			J=2			**69.4**	
Median			J=1			**86.6**	
			J=2			**54.5**	

Table 9. Photophysical parameters and B_{CPL} of CPL-active Yb-based compounds.

Yb	ε/$M^{-1}cm^{-1}$ (λ_{abs}/nm)	Φ	$\lvert g_{lum}\rvert$ (λ/nm)	B_{CPL} /$M^{-1}cm^{-1}$	Ref
Yb**L14**$(TTA)_3$	42000(345)	0.0062	0.019(970)	2.5	[121]
Yb**L16**$(TTA)_3$	52000(345)	0.0069	0.029(972)	5.2	[121]
Average				**3.75**	
Median				**3.75**	

3. Discussion

All the compound classes investigated show average B_{CPL} values in the order of magnitude of 10^1 - 10^2 range with the only exception of chiral ketones, exhibiting much lower values (in the order of 10^{-3}).The box plot reported in Figure 1 gives a general picture of the values and their distribution according to the data collected in the tables above. In general, the median B_{CPL} value, calculated for every class of CPL emitters, is much lower than the average. In the case of ketones, helicenes, pyrene excimers, d and f-metal compounds the average B_{CPL} falls even above the third quartile. This is an indication of a heavily tailed distribution with a strong positive skew, with most values falling on the lower end of the curve and few cases displaying exceptionally high B_{CPL}.

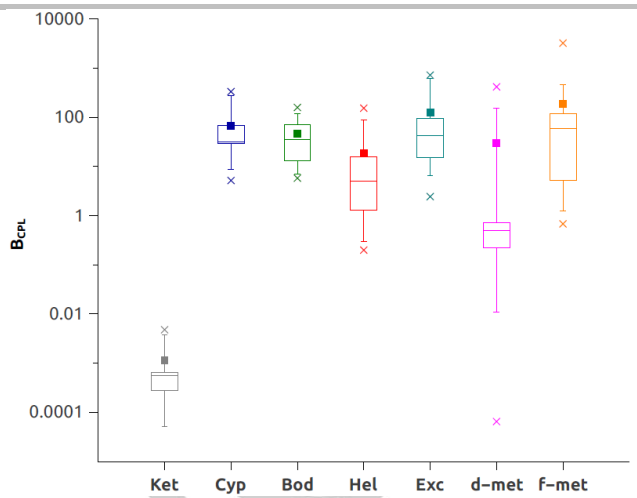

Figure 1. Box plot of B_{CPL} values for each class of CPL emitters taken into account in this work. Boxes represent the interquartile range, whiskers the 5^{th}-95^{th} percentile range, horizontal lines and the full dots median and average values respectively. Notice the Logarithmic vertical scale.

As expected, chiral ketones performances make them unsuitable for applications in CPL technologies where high overall efficiencies are needed, such as in CP-OLEDs. On the other hand, in the realm of purely organic compounds, cyclophanes, BODIPYs and particularly excimers offer higher-end CPL performances. Considered as a whole, d-metal compounds display rather scattered B_{CPL} values, partly due to the completely different nature of the metal involved (Cr, Ru, Re, Ir, Pt). Notably, Cr(III) compounds can reach very high B_{CPL} values in the NIR range (750 - 775 nm) at the blue-end edge of the NIR penetration window of biological tissues.

Extremely interesting values are offered by chiral lanthanide complexes which are able to feature transitions joining high g_{lum} with high quantum yields and absorption coefficients thanks to the antenna effect. Given these properties, on average and median, in terms of B_{CPL}, they outperform the state-of-art CPL emitting compounds, both purely organic and d-metal molecular systems. On the other hand, emission wavelengths of lanthanide complexes rigidly depend on the lanthanide ion itself, and apart from minor variations, they can not be modulated through ligand choice.

Interestingly, if the ground and emitting excited state of a compound has a similar geometry, then the g_{lum} and the g_{abs} associated with the most red-shifted transition in the electronic circular dichroism spectrum display similar magnitudes. Recently, Mori et al.[17,81] showed that this holds true in most cases for organic compounds. On the other hand, in the case of excimers and *f*-metal complexes (see above) completely different states are involved in absorption and emission and the rule can not apply.

Another important point to consider is the emission wavelength distribution of B_{CPL} values. Almost all the CPL emitters considered here display visible emission with an average global wavelength maximum falling in the green region (529 nm). A kernel density estimation of emission wavelength distribution is shown in Figure 2. Such curve shows a first maximum between 450 and 500 nm and a

second one around 600 nm, mostly due to Eu emitters. Most classes of emitters show high B_{CPL} performances in a relatively limited emission wavelength region, e.g. in the case of compounds giving rise to pyrene excimer, where emission is observed in the blue-greenish region. On the other hand, helicenes and helicenoids, despite their moderate B_{CPL} values, show emission all across the visible until the edge of the NIR region. Such high emission wavelength tunability is made possible by the multifarious extension and functionalization opportunities featured by helicene scaffolds.

In general, B_{CPL} is a metric of the total CPL signal available to be measured. According to the authors' experience, compounds with B_{CPL} > 1–10 $M^{-1}cm^{-1}$ display a CPL signal which can be relatively easily collected with most state-of-the-art spectrofluoropolarimeters. Indeed, if a compound displays high Φ (and ε), even signals associated with low g_{lum} (~10^{-4}) becomes accessible. Anyway, even in presence of a good instrumental signal, low g_{lum} factors always require a special care, as artifact signals due to linearly polarized light components can overwhelm true CPL. These considerations extend to the case of systems giving rise to a CPL signal upon interaction with an analyte, as in the case of CPL (bio)-assays.

Finally, beyond the molecular structural optimization, new ways to directly regulate the excited state and therefore to increase the CPL activity (g_{lum}) have been recently reported,[123] such as energy transfer amplified CPL,[124,125] chiral radical CPL[126] and photon upconversion.[127,128]

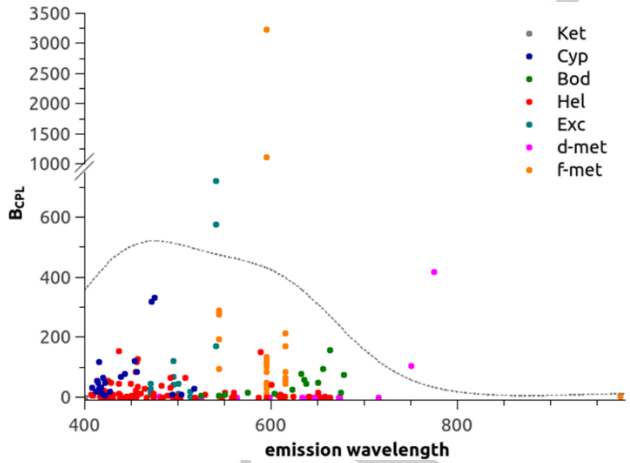

Figure 2. B_{CPL} values as a function of maximum emission wavelength (λ_{em}) for each compound reported in the tables above. The curve is a kernel density estimation of λ_{em} distribution (bandwith = 60 nm).

4. Conclusions

B_{CPL} is a value that can be readily calculated from experimental data. Such quantity yields a parameter directly proportional to the number of photons with a net circular polarization, gauging the overall detectable CPL signal. It can be conveniently used to compare CPL-active compounds with different photophysical properties and chemical nature. Researchers interested in designing, preparing or selecting CPL emitters for certain applications, such as CP fluorescence microscopy imaging, chiral photonics, etc., may focus in maximizing B_{CPL} instead of trying to maximize g_{lum} alone. Indeed, this survey may be useful to identify the parameters to optimize (ε, Φ or g_{lum}), within different compound classes, and where to invest synthetic efforts to obtain globally more performant CPL emitters.

Lorenzo Arrico obtained his PhD in "Chemistry and Materials Science" in 2020 under the supervision of Prof. Lorenzo Di Bari at the University of Pisa. His research activities have involved the preparation and the chiroptical investigation of both chiral organic systems and chiral metal complexes for the development of circularly polarized luminescence emitters.

Lorenzo Di Bari is Professor of Organic Chemistry at the University of Pisa, where since 2018 he's head of the Department of Chemistry and Industrial Chemistry. His research interests focus on the development of experimental methods for the stereochemistry of organic and inorganic compounds and on scouting novel applications of chiroptical properties.

Francesco Zinna obtained his PhD in 2016 under the supervision of Prof. Lorenzo Di Bari at the University of Pisa. Later, he spent a period at the University of Geneva (CH) in Prof. Jérôme Lacour's group as postdoctoral assistant. Since 2018, he has been assistant professor in the department of Chemistry and Industrial Chemistry at the University of Pisa. His scientific interests include preparation of chiral organic molecules and metal complexes, chiroptical studies of chiral systems focusing in particular on CPL properties and applications of CPL technologies in various fields such as chiral photonics and optoelectronics.

Acknowledgements

The University of Pisa is acknowledged for financial support. Dr Lorenzo Cupellini is thanked for helpful discussions.

Keywords: Circularly polarized luminescence • CPL • CP-OLED • chirality • lanthanides

References

[1] J. R. Brandt, F. Salerno, M. J. Fuchter, *Nat. Rev. Chem.* **2017**, *1*, 1.
[2] F. Zinna, U. Giovanella, L. Di Bari, *Adv. Mater.* **2015**, *27*, 1791.
[3] F. Zinna, M. Pasini, F. Galeotti, C. Botta, L. Di Bari, U. Giovanella, *Adv. Funct. Mater.* **2017**, *27*, 1603719.
[4] Y. Yang, R. C. da Costa, D.-M. Smilgies, A. J. Campbell, M. J. Fuchter, *Adv. Mater.* **2013**, *25*, 2624.
[5] J. R. Brandt, X. Wang, Y. Yang, A. J. Campbell, M. J. Fuchter, *J. Am. Chem. Soc.* **2016**, *138*, 9743.
[6] D. W. Zhang, M. Li, C. F. Chen, *Chem. Soc. Rev.* **2020**, *49*, 1331.
[7] R. Carr, N. H. Evans, D. Parker, *Chem. Soc. Rev.* **2012**, *41*, 7673.
[8] S. Orsini, F. Zinna, T. Biver, L. Di Bari, I. Bonaduce, *RSC Adv.* **2016**, *6*, 96176.
[9] L. E. MacKenzie, L. O. Pålsson, D. Parker, A. Beeby, R. Pal, *Nat. Commun.* **2020**, *11*, 1676.
[10] F. Zinna, L. Di Bari, *Chirality* **2015**, *27*, 1.
[11] T. Mori, in *Circ. Polariz. Lumin. Isol. Small Org. Mol.*, Springer Singapore, **2020**, pp. 1–10.
[12] *Circularly Polarized Luminescence of Isolated Small Organic Molecules* (Ed. T. Mori), Springer Singapore, **2020**.
[13] K. L. Wong, J. C. G. Bünzli, P. A. Tanner, *J. Lumin.* **2020**, *224*, 117256.
[14] F. Zinna, Circularly Polarized Luminescence: From Spectroscopy to Applications, PhD Thesis, University of Pisa, **2016**.
[15] F. Zinna, L. Di Bari, in *Lanthanide-Based Multifunct. Mater. From OLEDs to SIMs*, Elsevier, **2018**, pp. 171–194.
[16] T. Mori, in *Circ. Polariz. Lumin. Isol. Small Org. Mol.*, Springer Singapore, **2020**, pp. 1–10.
[17] Y. Nagata, T. Mori, *Front. Chem.* **2020**, *8*, 448.
[18] E. M. Sánchez-Carnerero, A. R. Agarrabeitia, F. Moreno, B. L. Maroto, G. Muller, M. J. Ortiz, S. de la Moya, *Chem. - A Eur. J.* **2015**, *21*, 13488.
[19] C. A. Emeis, L. J. Oosterhoff, *Chem. Phys. Lett.* **1967**, *1*, 129.
[20] P. H. Schippers, J. P. M. van der Ploeg, H. P. J. M. Dekkers, *J. Am. Chem. Soc.* **1983**, *105*, 84.
[21] M. Gon, Y. Morisaki, Y. Chujo, *Chem. Commun.* **2017**, *53*, 8304.
[22] M. Gon, Y. Morisaki, Y. Chujo, *Chem. - A Eur. J.* **2017**, *23*, 6323.
[23] M. Gon, Y. Morisaki, Y. Chujo, *European J. Org. Chem.* **2015**, *2015*, 7756.
[24] M. Gon, Y. Morisaki, Y. Chujo, *J. Mater. Chem. C* **2015**, *3*, 521.
[25] M. Gon, Y. Morisaki, R. Sawada, Y. Chujo, *Chem. - A Eur. J.* **2016**, *22*, 2291.
[26] Y. Morisaki, K. Inoshita, Y. Chujo, *Chem. - A Eur. J.* **2014**, *20*, 8386.
[27] Y. Morisaki, R. Sawada, M. Gon, Y. Chujo, *Chem. - An Asian J.* **2016**, *11*, 2524.
[28] T. Gao, H. He, R. Huang, M. Zheng, F. F. Wang, Y. J. Hu, F. L. Jiang, Y. Liu, *Dye. Pigment.* **2017**, *141*, 530.
[29] F. Zinna, T. Bruhn, C. A. Guido, J. Ahrens, M. Bröring, L. Di Bari, G. Pescitelli, *Chem. - A Eur. J.* **2016**, *22*, 16089.
[30] M. Saikawa, T. Nakamura, J. Uchida, M. Yamamura, T. Nabeshima, *Chem. Commun.* **2016**, *52*, 10727.
[31] C. Ray, E. M. Sánchez-Carnerero, F. Moreno, B. L. Maroto, A. R. Agarrabeitia, M. J. Ortiz, Í. López-Arbeloa, J. Bañuelos, K. D. Cohovi, J. L. Lunkley, G. Muller, S. de la Moya, *Chem. - A Eur. J.* **2016**, *22*, 8805.
[32] R. B. Alnoman, S. Rihn, D. C. O'Connor, F. A. Black, B. Costello, P. G. Waddell, W. Clegg, R. D. Peacock, W. Herrebout, J. G. Knight, M. J. Hall, *Chem. - A Eur. J.* **2016**, *22*, 93.
[33] E. M. Sánchez-Carnerero, F. Moreno, B. L. Maroto, A. R. Agarrabeitia, M. J. Ortiz, B. G. Vo, G. Muller, S. D. La Moya, *J. Am. Chem. Soc.* **2014**, *136*, 3346.
[34] R. Clarke, K. L. Ho, A. A. Alsimaree, O. J. Woodford, P. G. Waddell, J. Bogaerts, W. Herrebout, J. G. Knight, R. Pal, T. J. Penfold, M. J. Hall, *ChemPhotoChem* **2017**, *1*, 513.
[35] J. Jiménez, L. Cerdán, F. Moreno, B. L. Maroto, I. García-Moreno, J. L. Lunkley, G. Muller, S. De La Moya, *J. Phys. Chem. C* **2017**, *121*, 5287.
[36] K. Dhbaibi, L. Favereau, J. Crassous, *Chem. Rev.* **2019**, *119*, 8846.
[37] W. L. Zhao, M. Li, H. Y. Lu, C. F. Chen, *Chem. Commun.* **2019**, *55*, 13793.
[38] L. Fang, M. Li, W. Lin, Y. Shen, C. Chen, *Asian J. Org. Chem.* **2018**, *7*, 2518.
[39] H. Tanaka, Y. Kato, M. Fujiki, Y. Inoue, T. Mori, *J. Phys. Chem. A* **2018**, *122*, 7378.
[40] L. Fang, M. Li, W. Bin Lin, C. F. Chen, *Tetrahedron* **2018**, *74*, 7164.
[41] L. Fang, M. Li, W. Bin Lin, Y. Shen, C. F. Chen, *J. Org. Chem.* **2017**, *82*, 7402.
[42] Z. Ma, T. Winands, N. Liang, D. Meng, W. Jiang, N. L. Doltsinis, Z. Wang, *Sci. China Chem.* **2020**, *63*, 208.
[43] H. Sakai, T. Kubota, J. Yuasa, Y. Araki, T. Sakanoue, T. Takenobu, T. Wada, T. Kawai, T. Hasobe, *J. Phys. Chem. C* **2016**, *120*, 7860.
[44] N. Saleh, M. Srebro, T. Reynaldo, N. Vanthuyne, L. Toupet, V. Y. Chang, G. Muller, J. A. G. Williams, C. Roussel, J. Autschbach, J. Crassous, *Chem. Commun.* **2015**, *51*, 3754.
[45] N. Saleh, B. Moore, M. Srebro, N. Vanthuyne, L. Toupet, J. A. G. Williams, C. Roussel, K. K. Deol, G. Muller, J. Autschbach, J. Crassous, *Chem. - A Eur. J.* **2015**, *21*, 1673.
[46] C. Shen, E. Anger, M. Srebro, N. Vanthuyne, K. K. Deol, T. D. Jefferson, G. Muller, J. A. G. Williams, L. Toupet, C. Roussel, J. Autschbach, R. Réau, J. Crassous, *Chem. Sci.* **2014**, *5*, 1915.
[47] K. Dhbaibi, L. Favereau, M. Srebro-Hooper, C. Quinton, N. Vanthuyne, L. Arrico, T. Roisnel, B. Jamoussi, C. Poriel, C. Cabanetos, J. Autschbach, J. Crassous, *Chem. Sci.* **2020**, *11*, 567.
[48] C. Schaack, L. Arrico, E. Sidler, M. Górecki, L. Di Bari, F. Diederich, *Chem. – A Eur. J.* **2019**, *25*, 8003.
[49] C. Schaack, E. Sidler, N. Trapp, F. Diederich, *Chem. - A Eur. J.* **2017**, *23*, 14153.
[50] K. Dhbaibi, L. Favereau, M. Srebro-Hooper, M. Jean, N. Vanthuyne, F. Zinna, B. Jamoussi, L. Di Bari, J. Autschbach, J. Crassous, *Chem. Sci.* **2018**, *9*, 735.
[51] H. Sakai, S. Shinto, J. Kumar, Y. Araki, T. Sakanoue, T. Takenobu, T. Wada, T. Kawai, T. Hasobe, *J. Phys. Chem. C* **2015**, *119*, 13937.
[52] K. Yavari, W. Delaunay, N. De Rycke, T. Reynaldo, P. Aillard, M. Srebro-Hooper, V. Y. Chang, G. Muller, D. Tondelier, B. Geffroy, A. Voituriez, A. Marinetti, M. Hissler, J. Crassous, *Chem. – A Eur. J.* **2019**, *25*, 5303.
[53] R. Yamano, J. Hara, K. Murayama, H. Sugiyama, K. Teraoka, H. Uekusa, S. Kawauchi, Y. Shibata, K. Tanaka, *Org. Lett.* **2017**, *19*, 42.
[54] R. Yamano, Y. Shibata, K. Tanaka, *Chem. – A Eur. J.* **2018**, *24*, 6364.
[55] C. Maeda, K. Nagahata, T. Shirakawa, T. Ema, *Angew. Chemie Int. Ed.* **2020**, *59*, 7813.
[56] H. Oyama, M. Akiyama, K. Nakano, M. Naito, K. Nobusawa, K. Nozaki, *Org. Lett.* **2016**, *18*, 3654.
[57] T. Otani, A. Tsuyuki, T. Iwachi, S. Someya, K. Tateno, H. Kawai, T. Saito, K. S. Kanyiva, T. Shibata, *Angew. Chemie Int. Ed.* **2017**, *56*, 3906.
[58] K. Goto, R. Yamaguchi, S. Hiroto, H. Ueno, T. Kawai, H. Shinokubo, *Angew. Chemie Int. Ed.* **2012**, *51*, 10333.
[59] T. Matsuno, Y. Koyama, S. Hiroto, J. Kumar, T. Kawai, H. Shinokubo, *Chem. Commun.* **2015**, *51*, 4607.
[60] T. Otani, T. Sasayama, C. Iwashimizu, K. S. Kanyiva, H. Kawai, T. Shibata, *Chem. Commun.* **2020**, *56*, 4484.
[61] Y. Sawada, S. Furumi, A. Takai, M. Takeuchi, K. Noguchi, K. Tanaka, *J. Am. Chem. Soc.* **2012**, *134*, 4080.
[62] S. Nishigaki, K. Murayama, Y. Shibata, K. Tanaka, *Mater. Chem. Front.* **2018**, *2*, 585.
[63] Y. Yamamoto, H. Sakai, J. Yuasa, Y. Araki, T. Wada, T. Sakanoue, T. Takenobu, T. Kawai, T. Hasobe, *J. Phys. Chem. C* **2016**, *120*, 7421.
[64] Y. Yamamoto, H. Sakai, J. Yuasa, Y. Araki, T. Wada, T. Sakanoue, T. Takenobu, T. Kawai, T. Hasobe, *Chem. - A Eur. J.* **2016**, *22*, 4263.
[65] L. Guy, M. Mosser, D. Pitrat, J. C. Mulatier, M. Kukułka, M. Srebro-Hooper, E. Jeanneau, A. Bensalah-Ledoux, B. Baguenard, S. Guy, *J. Org. Chem.* **2019**, *84*, 10870.
[66] H. Isla, M. Srebro-Hooper, M. Jean, N. Vanthuyne, T. Roisnel, J. L. Lunkley, G. Muller, J. A. G. Williams, J. Autschbach, J. Crassous, *Chem. Commun.* **2016**, *52*, 5932.
[67] H. Isla, N. Saleh, J. K. Ou-Yang, K. Dhbaibi, M. Jean, M. Dziurka, L. Favereau, N. Vanthuyne, L. Toupet, B. Jamoussi, M. Srebro-Hooper, J. Crassous, *J. Org. Chem.* **2019**, *84*, 5383.
[68] A. Ushiyama, S. Hiroto, J. Yuasa, T. Kawai, H. Shinokubo, *Org. Chem. Front.* **2017**, *4*, 664.
[69] M. Satoh, Y. Shibata, K. Tanaka, *Chem. – A Eur. J.* **2018**, *24*, 5434.
[70] K. Nakamura, S. Furumi, M. Takeuchi, T. Shibuya, K. Tanaka, *J. Am. Chem. Soc.* **2014**, *136*, 5555.
[71] Z. Domínguez, R. López-Rodríguez, E. Álvarez, S. Abbate, G. Longhi, U. Pischel, A. Ros, *Chem. - A Eur. J.* **2018**, *24*, 12660.
[72] C. Shen, M. Srebro-Hooper, M. Jean, N. Vanthuyne, L. Toupet, J. A. G. Williams, A. R. Torres, A. J. Riives, G. Muller, J. Autschbach, J. Crassous, *Chem. - A Eur. J.* **2017**, *23*, 407.
[73] Z. H. Zhao, X. Liang, M. X. He, M. Y. Zhang, C. H. Zhao, *Org. Lett.* **2019**, *21*, 9569.
[74] H. Oyama, K. Nakano, T. Harada, R. Kuroda, M. Naito, K. Nobusawa, K. Nozaki, *Org. Lett.* **2013**, *15*, 2104.
[75] T. Katayama, S. Nakatsuka, H. Hirai, N. Yasuda, J. Kumar, T. Kawai, T. Hatakeyama, *J. Am. Chem. Soc.* **2016**, *138*, 5210.
[76] K. Murayama, Y. Oike, S. Furumi, M. Takeuchi, K. Noguchi, K. Tanaka, *European J. Org. Chem.* **2015**, *2015*, 1409.
[77] S. Pascal, C. Besnard, F. Zinna, L. Di Bari, B. Le Guennic, D. Jacquemin, J. Lacour, *Org. Biomol. Chem.* **2016**, *14*, 4590.
[78] R. Duwald, J. Bosson, S. Pascal, S. Grass, F. Zinna, C. Besnard, L. Di Bari, D. Jacquemin, J. Lacour, *Chem. Sci.* **2020**, *11*, 1165.
[79] J. Bosson, G. M. Labrador, S. Pascal, F.-A. Miannay, O. Yushchenko, H. Li, L. Bouffier, N. Sojic, R. C. Tovar, G. Muller, D. Jacquemin, A. D. Laurent, B. Le Guennic, E. Vauthey, J. Lacour, *Chem. - A Eur. J.* **2016**, *22*, 18394.
[80] I. H. Delgado, S. Pascal, A. Wallabregue, R. Duwald, C. Besnard, L. Guénée, C. Nançoz, E. Vauthey, R. C. Tovar, J. L. Lunkley, G. Muller, J. Lacour, *Chem. Sci.* **2016**, *7*, 4685.
[81] H. Tanaka, Y. Inoue, T. Mori, *ChemPhotoChem* **2018**, *2*, 386.
[82] F. Zinna, E. Brun, A. Homberg, J. Lacour, in *Circ. Polariz. Lumin. Isol. Small Org. Mol.*, Springer Singapore, **2020**, pp. 273–292.
[83] J. Duhamel, *Langmuir* **2012**, *28*, 6527.
[84] S. Nakanishi, K. Nakabayashi, T. Mizusawa, N. Suzuki, S. Guo, M. Fujiki, Y. Imai, *RSC Adv.* **2016**, *6*, 99172.
[85] N. Hara, K. Okuda, M. Shizuma, N. Tajima, Y. Imai, *ChemistrySelect* **2019**, *4*, 10209.
[86] Y. Hashimoto, T. Nakashima, D. Shimizu, T. Kawai, *Chem. Commun.*

2016, *52*, 5171.
[87] A. Homberg, E. Brun, F. Zinna, S. Pascal, M. Górecki, L. Monnier, C. Besnard, G. Pescitelli, L. Di Bari, J. Lacour, *Chem. Sci.* **2018**, *9*, 7043.
[88] S. Ito, K. Ikeda, S. Nakanishi, Y. Imai, M. Asami, *Chem. Commun.* **2017**, *53*, 6323.
[89] K. Takaishi, R. Takehana, T. Ema, *Chem. Commun.* **2018**, *54*, 1449.
[90] F. Zinna, S. Voci, L. Arrico, E. Brun, A. Homberg, L. Bouffier, T. Funaioli, J. Lacour, N. Sojic, L. Di Bari, *Angew. Chemie* **2019**, *131*, 7026.
[91] A. D. Kirk, G. B. Porter, *J. Phys. Chem.* **1980**, *84*, 887.
[92] J. R. Jiménez, B. Doistau, C. M. Cruz, C. Besnard, J. M. Cuerva, A. G. Campaña, C. Piguet, *J. Am. Chem. Soc.* **2019**, *141*, 13244.
[93] C. Dee, F. Zinna, W. R. Kitzmann, G. Pescitelli, K. Heinze, L. Di Bari, M. Seitz, *Chem. Commun.* **2019**, *55*, 13078.
[94] P. M. L. Blok, P. S. Cartwright, H. P. J. M. Dekkers, R. D. Gillard, *J. Chem. Soc. Chem. Commun.* **1987**, 1232.
[95] K. Suzuki, A. Kobayashi, S. Kaneko, K. Takehira, T. Yoshihara, H. Ishida, Y. Shiina, S. Oishi, S. Tobita, *Phys. Chem. Chem. Phys.* **2009**, *11*, 9850.
[96] A. Gafni, I. Z. Steinberg, *Isr. J. Chem.* **1976**, *15*, 102.
[97] K. Nakamaru, *Bull. Chem. Soc. Jpn.* **1982**, *55*, 2697.
[98] N. Hellou, M. Srebro-Hooper, L. Favereau, F. Zinna, E. Caytan, L. Toupet, V. Dorcet, M. Jean, N. Vanthuyne, J. A. G. Williams, L. Di Bari, J. Autschbach, J. Crassous, *Angew. Chemie Int. Ed.* **2017**, *56*, 8236.
[99] T. Biet, T. Cauchy, Q. Sun, J. Ding, A. Hauser, P. Oulevey, T. Bürgi, D. Jacquemin, N. Vanthuyne, J. Crassous, N. Avarvari, *Chem. Commun.* **2017**, *53*, 9210.
[100] X. P. Zhang, L. L. Wang, X. W. Qi, D. S. Zhang, Q. Y. Yang, Z. F. Shi, Q. Lin, T. Wu, *Dalt. Trans.* **2018**, *47*, 10179.
[101] N. Sojic, S. Voci, F. Zinna, L. Arrico, S. Grass, L. Bouffier, J. Lacour, L. Di Bari, *Chem. Commun.* **2020**, DOI 10.1039/d0cc01571g.
[102] J. C. G. Bünzli, C. Piguet, *Chem. Soc. Rev.* **2005**, *34*, 1048.
[103] F. Zinna, U. Giovanella, L. Di Bari, *Adv. Mater.* **2015**, *27*, 1791.
[104] J. L. Lunkley, D. Shirotani, K. Yamanari, S. Kaizaki, G. Muller, *Inorg. Chem.* **2011**, *50*, 12724.
[105] A. Taniguchi, N. Hara, M. Shizuma, N. Tajima, M. Fujiki, Y. Imai, *Photochem. Photobiol. Sci.* **2019**, *18*, 2859.
[106] S. Wada, Y. Kitagawa, T. Nakanishi, K. Fushimi, Y. Morisaki, K. Fujita, K. Konishi, K. Tanaka, Y. Chujo, Y. Hasegawa, *NPG Asia Mater.* **2016**, *8*, e251.
[107] S. Petoud, G. Muller, E. G. Moore, J. Xu, J. Sokolnicki, J. P. Riehl, U. N. Le, S. M. Cohen, K. N. Raymond, *J. Am. Chem. Soc.* **2007**, *129*, 77.
[108] M. Lama, O. Mamula, G. S. Kottas, F. Rizzo, L. De Cola, A. Nakamura, R. Kuroda, H. Stoeckli-Evans, *Chem. - A Eur. J.* **2007**, *13*, 7358.
[109] M. Seitz, E. G. Moore, A. J. Ingram, G. Muller, K. N. Raymond, *J. Am. Chem. Soc.* **2007**, *129*, 15468.
[110] F. S. Richardson, *Inorg. Chem.* **1980**, *19*, 2806.
[111] N. Hara, M. Okazaki, M. Shizuma, S. Marumoto, N. Tajima, M. Fujiki, Y. Imai, *ChemistrySelect* **2017**, *2*, 10317.
[112] O. Kotova, S. Blasco, B. Twamley, J. O'Brien, R. D. Peacock, J. A. Kitchen, M. Martínez-Calvo, T. Gunnlaugsson, *Chem. Sci.* **2015**, *6*, 457.
[113] M. Hasegawa, D. Iwasawa, T. Kawaguchi, H. Koike, A. Saso, S. Ogata, A. Ishii, H. Ohmagari, M. Iwamura, K. Nozaki, *Chempluschem* **2020**, *85*, 294.
[114] M. Górecki, L. Carpita, L. Arrico, F. Zinna, L. Di Bari, *Dalt. Trans.* **2018**, *47*, 7166.
[115] M. Starck, L. E. Mackenzie, A. S. Batsanov, D. Parker, R. Pal, *Chem. Commun.* **2019**, *55*, 14115.
[116] A. T. Frawley, R. Pal, D. Parker, *Chem. Commun.* **2016**, *52*, 13349.
[117] S. J. Butler, M. Delbianco, N. H. Evans, A. T. Frawley, R. Pal, D. Parker, R. S. Puckrin, D. S. Yufit, *Dalt. Trans.* **2014**, *43*, 5721.
[118] D. Liu, Y. Zhou, Y. Zhang, H. Li, P. Chen, W. Sun, T. Gao, P. Yan, *Inorg. Chem.* **2018**, *57*, 8332.
[119] Y. Zhou, H. Li, T. Zhu, T. Gao, P. Yan, *J. Am. Chem. Soc.* **2019**, *141*, 19634.
[120] C. L. Maupin, D. Parker, J. A. G. Williams, J. P. Riehl, *J. Am. Chem. Soc.* **1998**, *120*, 10563.
[121] F. Zinna, L. Arrico, L. Di Bari, *Chem. Commun.* **2019**, *55*, 6607.
[122] C. L. Maupin, R. S. Dickins, L. G. Govenlock, C. E. Mathieu, D. Parker, J. A. Gareth Williams, J. P. Riehl, *J. Phys. Chem. A* **2000**, *104*, 6709.
[123] T. Zhao, J. Han, P. Duan, M. Liu, *Acc. Chem. Res.* **2020**, *53*, 1279.
[124] D. Yang, P. Duan, L. Zhang, M. Liu, *Nat. Commun.* **2017**, *8*, 1.
[125] L. Ji, Y. Sang, G. Ouyang, D. Yang, P. Duan, Y. Jiang, M. Liu, *Angew. Chemie Int. Ed.* **2019**, *58*, 844.
[126] Y. Wang, Y. Jiang, X. Zhu, M. Liu, *J. Phys. Chem. Lett.* **2019**, *10*, 5861.
[127] J. Han, P. Duan, X. Li, M. Liu, *J. Am. Chem. Soc.* **2017**, *139*, 9783.
[128] T. Zhao, J. Han, X. Qin, M. Zhou, P. Duan, *J. Phys. Chem. Lett.* **2020**, *11*, 311.

Entry for the Table of Contents

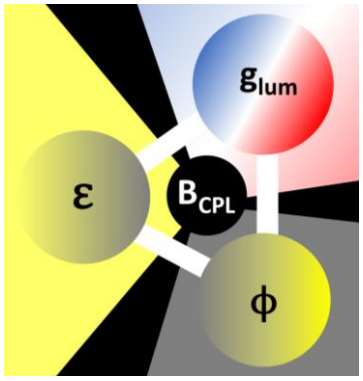

A new tool, named CPL brightness (B_{CPL}), is introduced to evaluate the performances of CPL emitters. Beyond the dissymmetry factor, it takes into account quantum yields and extinction coefficients, allowing an easy and direct comparison of various CPL-emitters belonging to different chemical classes.

Institute and/or researcher Twitter usernames: ((optional))